ขั้วไฟฟ้าดัดแปรไมเซลลาร์แกรฟีนออกไซด์ที่ถูกรีดิวซ์ทางเคมีไฟฟ้าสำหรับการตรวจวัดคาร์โบฟิวแรน และคาร์เบนดาซิมในคราวเดียวกัน

นายนลทพล อัครชาญชัยนนท์

วิทยานิพนธ์นี้เป็นส่วนหนึ่งของการศึกษาตามหลักสูตรปริญญาวิทยาศาสตรมหาบัณฑิต
สาขาวิชาเคมี ภาควิชาเคมี
คณะวิทยาศาสตร์ จุฬาลงกรณ์มหาวิทยาลัย
ปีการศึกษา 2558

ELECTROCHEMICALLY REDUCED MICELLAR GRAPHENE OXIDE MODIFIED ELECTRODE FOR SIMULTANEOUS DETECTION OF CARBOFURAN AND CARBENDAZIM

Mr. Nontapol Akkarachanchainon

A Thesis Submitted in Partial Fulfillment of the Requirements
for the Degree of Master of Science Program in Chemistry
Department of Chemistry
Faculty of Science
Chulalongkorn University
Academic Year 2015

Thesis Title	ELECTROCHEMICALLY REDUCED MICELLAR GRAPHENE OXIDE MODIFIED ELECTRODE FOR SIMULTANEOUS DETECTION OF CARBOFURAN AND CARBENDAZIM
By	Mr. Nontapol Akkarachanchainon
Field of Study	Chemistry
Thesis Advisor	Professor Orawon Chailapakul, Ph.D.
Thesis Co-Advisor	Nadnudda Rodthongkum, Ph.D.

Accepted by the Faculty of Science, Chulalongkorn University in Partial Fulfillment of the Requirements for the Master's Degree

.....Dean of the Faculty of Science
(Associate Professor Polkit Sangvanich, Ph.D.)

THESIS COMMITTEE

.....Chairman
(Associate Professor Vudhichai Parasuk, Ph.D.)

.....Thesis Advisor
(Professor Orawon Chailapakul, Ph.D.)

.....Thesis Co-Advisor
(Nadnudda Rodthongkum, Ph.D.)

.....Examiner
(Assistant Professor Suchada Chuanuwatanakul, Ph.D.)

.....Examiner
(Associate Professor Nattaya Ngamrojanavanich, Ph.D.)

.....External Examiner
(Associate Professor Weena Siangproh, Ph.D.)

นลทพล อัครชาญชัยนนท์ : ขั้วไฟฟ้าดัดแปรไมเซลลาร์แกรฟีนออกไซด์ที่ถูกรีดิวซ์ทางเคมีไฟฟ้าสำหรับการตรวจวัดคาร์โบฟิวแรนและคาร์เบนคาซิมในคราวเดียวกัน (ELECTROCHEMICALLY REDUCED MICELLAR GRAPHENE OXIDE MODIFIED ELECTRODE FOR SIMULTANEOUS DETECTION OF CARBOFURAN AND CARBENDAZIM) อ.ที่ปรึกษาวิทยานิพนธ์หลัก: ศ. ดร.อรวรรณ ชัยลภากุล, อ.ที่ปรึกษาวิทยานิพนธ์ร่วม: ดร.นาฏนัดดา รอดทองคำ, 82 หน้า.

แกรฟีนซึ่งเป็นสารที่มีโครงสร้างเป็นระนาบเดี่ยวของแกรไฟต์ จัดว่าเป็นหนึ่งในวัสดุนาโนที่มีคาร์บอนเป็นองค์ประกอบหลักซึ่งได้รับความนิยมสำหรับนำไปดัดแปรขั้วไฟฟ้าเพื่อใช้เป็นตัวรับรู้ทางเคมีไฟฟ้า เนื่องจากการมีสมบัติที่โดดเด่นทางด้านเคมีไฟฟ้า อย่างไรก็ตามด้วยสมบัติความไม่ชอบน้ำของแกรฟีนจึงทำให้ผิวสัมผัสเข้ากับน้ำได้ไม่ดี ซึ่งส่งผลกีดขวางต่อกระบวนการส่งผ่านอิเล็กตรอน ในงานวิจัยนี้ได้ปรับเปลี่ยนสมบัติของแกรฟีนที่ใช้เป็นขั้วไฟฟ้าให้มีความชอบน้ำโดยใช้วิธีดัดแปรพื้นผิวไมเซลล์ของแกรฟีนออกไซด์ด้วยเทคนิคทางเคมีไฟฟ้า จากนั้นจึงนำขั้วไฟฟ้าดังกล่าวไปประยุกต์ใช้ในการตรวจวัดคาร์โบฟูแรนและคาร์เบนดาซิมโดยทำการตรวจวัดสารทั้งสองชนิดไปพร้อมกัน เป็นที่น่าสนใจว่า ขั้วไฟฟ้าดัดแปรที่ได้จากงานวิจัยนี้ให้ความไวของการตรวจวัดทางเคมีไฟฟ้าที่สูงขึ้นโดยพิสูจน์ได้จากค่าสัญญาณกระแสของคาร์โบฟูแรนและคาร์เบนดาซิมที่เพิ่มขึ้นถึง 4 เท่าและ 12 เท่าตามลำดับเมื่อเทียบกับขั้วไฟฟ้าที่ไม่ได้ดัดแปร ทั้งนี้ภายใต้ภาวะที่เหมาะสมพบว่า ขีดจำกัดของการตรวจวัดคาร์โบฟูแรนและคาร์เบนดาซิมสามารถตรวจวัดได้ในระดับต่ำถึง 10 ไมโครกรัมต่อลิตร และ 5 ไมโครกรัมต่อลิตร โดยมีช่วงความเป็นเส้นตรงอยู่ที่ระดับความเข้มข้น 40 ถึง 20,000 ไมโครกรัมต่อลิตร และ 25 ถึง 5,000 ไมโครกรัมต่อลิตรตามลำดับ นอกจากนี้ยังพบว่า ขั้วไฟฟ้าแกรฟีนดัดแปรดังกล่าวสามารถนำไปประยุกต์ใช้ในการตรวจวัดคาร์โบฟูแรนและคาร์เบนดาซิมที่ตกค้างในผลผลิตจริงทางการเกษตรได้

ภาควิชา เคมี	ลายมือชื่อนิสิต .....
สาขาวิชา เคมี	ลายมือชื่อ อ.ที่ปรึกษาหลัก .....
ปีการศึกษา 2558	ลายมือชื่อ อ.ที่ปรึกษาร่วม .....

5671997323 : MAJOR CHEMISTRY
KEYWORDS: ELECTROCHEMICALLY REDUCED MICELLAR GRAPHENE OXIDE / ELECTROCHEMICAL DETECTION / GRAPHENE OXIDE / CARBOFURAN / CARBENDAZIM

NONTAPOL AKKARACHANCHAINON: ELECTROCHEMICALLY REDUCED MICELLAR GRAPHENE OXIDE MODIFIED ELECTRODE FOR SIMULTANEOUS DETECTION OF CARBOFURAN AND CARBENDAZIM. ADVISOR: PROF. ORAWON CHAILAPAKUL, Ph.D., CO-ADVISOR: NADNUDDA RODTHONGKUM, Ph.D., 82 pp.

Graphene, an isolated single layer of graphite, is one of the well-publicized carbon based nanomaterials used for electrode modification in electrochemical sensor due to its outstanding electrochemical properties. However, hydrophobicity of graphene makes it incompatible with aqueous solution, leading to impediment to electron transfer process. Here, we alter graphene property to be hydrophilicity by using electrochemically reduced micellar graphene oxide for electrode surface modification. Then, this system was applied for the simultaneous determination of carbofuran and carbendazim. Interestingly, the modified electrode offers an improved electrochemical sensitivity, verified by a drastic increase in current signal of carbofuran (4 times) and carbendazim (12 times) compared with unmodified electrode. Under the optimal conditions, low detection limits of carbofuran and carbendazim were found to be 10 μg L^{-1} and 5 μg L^{-1} with the wide linear ranges of 40-20,000 μg $L^{-1}$and 25-5,000 μg L^{-1}, respectively. Ultimately, this approach was successfully applied for sensitive determination of carbofuran and carbendazim residues in real agricultural products.

Department:	Chemistry	Student's Signature	.....
Field of Study:	Chemistry	Advisor's Signature	.....
Academic Year:	2015	Co-Advisor's Signature	.....

ACKNOWLEDGEMENTS

I would like to thank all my thesis adviser and co-adviser including Professor Dr. Orawon Chailapakul and Dr. Nadnudda Rodthogkum for their useful advice and encouragement throughout the thesis.

I am grateful to all thesis committee members including Associate Professor Dr. Vudhichai Parasuk, Assistance Professor Dr. Suchada Chuanuwatanakul, Assistance Professor Dr. Nattaya Ngamrojanavanich and Assistance Professor Dr. Weena Siangproh for their comments and interesting advice.

I would like to appreciate the financial supports from Center of Excellence on Petrochemical and Materials Technology (PETROMAT) through High Performance and Smart Materials (HPSM) research program.

I am also thankful for warm friendship and great motivation from all my group members.

Finally, I would like to thank my family for their love and encouragement throughout my entire life.

CONTENTS

Page

Page

Page

Page

LIST OF FIGURES

Page

LIST OF TABLES

Page

CHAPTER I
INTRODUCTION

1.1 Introduction

One of the current environmental problems which our world is confronting is the contamination of natural resources, particularly in an issue of residual pesticide contaminants. There is no gainsaying that some noxious pesticides have been widely used around the world. Carbofuran and carbendazim, commonly used as insecticide and fungicide, are considered as the most hazardous pesticides. Both of them have potential to wreak widespread destruction of natural environment. With inadvertent use of them, there will be inevitable contamination in air, food and water sources and adversely impact through living organism food chain [1]. Consequently, they not only devastate wildlife, but also severely harm human health. Carbofuran (CBF) is known as one of the most toxic carbamate insecticide due to its high insecticidal activity. It is used to control insects in crop fields. On the other hand, carbendazim (CBZ), a benzimidazole based fungicide, is extensively employed for wild range of plant disease control. It is considered as a highly toxic chemical because carbendazim possesses long degradation time due to its unbreakable chemical structure. Owing to the widespread use in agriculture, the pesticide residues potentially contaminate in various agricultural products. A large amount of intake tends to accumulate in human body and could be fatal. Furthermore, it has been reported that carbofuran and carbendazim are the carcinogenic substances causing chronic and acute disease [2-4]. Therefore, sensitive and accurate method for the detection of these pesticides is important to control as well as protect the environmental contamination.

There are several conventional analytical methods commonly used for CBF and CBZ determination, such as ultraviolet spectroscopy [5], spectrophotometry [6], gas chromatography [7], high-performance liquid chromatography [8, 9] and capillary electrophoresis [10] *etc*. Unfortunately, these techniques still have some drawbacks, for example, high operating cost, non-portability, long analysis time, requirement of skilled technicians, complicated sample pretreatment and use of toxic organic solvent.

Thus, electrochemical technique has become an interesting and alternative option due to its inexpensiveness, fast analysis and portability; however, the performance of conventional electrodes has still not sufficed to accomplish the sensitive analyses. To unravel this problem, modification of electrode surface is a crucial step. In the recent years, electrochemical biosensors were used for CBF and CBZ detection using electrochemical detection based on specific enzyme activities; however, these systems have a lot of disadvantages, such as high cost, relatively poor stability and reproducibility and requirement of pretreatment step. Thereby, considerable attentions have been focused on non-enzymatic based electrochemical system as an alternative approach.

The advent of nanoscience and nanotechnology has brought exceedingly beneficial applications in the fields of science. The nanoscopic-scale materials have been widely used in many research areas, including analytical chemistry. Various types of nanomaterials, such as metallic nanoparticles [11, 12], carbon based nanomaterials (*i.e.* fullerenes [13], carbon nanofibers [14], carbon nanotubes [15], carbon nanodots [16], graphene) have been used for electrode surface modification. Among all, graphene (G) [17, 18], one of the carbon based nanomaterials, has become contemporarily promising material in several applications. G is an allotrope of carbon which made up from entire sp^2-carbon lattice structure arranged in 2-dimensional single-layer sheet. Due to its attractive properties, such as large surface area, high electron transfer and excellent electrical conductivity, it is a notable material which is suitable for electrode modification.

However, G has an unfavorable difficulty due to strong Van der Waals interactions among the neighboring sheets. Thus, G usually suffers from a severe tendency of self-agglomeration and re-stacking, being a cause of loss in effective surface area and conductivity. Therefore, it is necessary to prevent self- agglomeration of G. Alternatively, graphene oxide (GO) has similar structure to G, but the difference is the decoration of oxygen functional groups on the plane of carbon atoms. An important property of GO is well dispersibility in water due to its high polarity of oxygen functionalities. On the contrary, in terms of electrical property, GO is often classified

as an electrical insulator because of the disruption from the oxygen functional groups on its structure. Therefore, GO is used as a precursor and reduced into pristine G by removal of oxygen-containing groups on GO with reduction reaction. GO which is reduced in to G is called reduced graphene oxide (RGO). There are several methods [19-22] to achieve reduction reaction based on chemical reduction, thermal reduction or electrochemical reduction. From the previous literatures [23], although RGO using chemical reduction is a large scale method, but this method has caused contamination of reducing agents in RGO solution as a result of poor-quality yields. Likewise, for thermal reduction at high temperature, this method can produce very high surface area RGO, but the heating process can damage the structure of RGO sheets [24]. Nonetheless, GO which is reduced by electrochemical method, denoted as electrochemically reduced graphene oxide (ERGO) [25, 26], can be created as the best quality compared to others. Unfortunately, as soon as GO was reduced to G, the decorated oxygen functionalities will be removed instantaneously. The planar structure of G remains merely entire carbon structure, so it is classified as a hydrophobic material. Inevitably, G surface repels aqueous solution. In this work, we aim to adjust a property of graphene surface to be hydrophilic by simply using of common surfactant for improving its interfacial property.

Surfactants are the surface-active compounds consisting of hydrophilic heads on one side and long chain hydrophobic tails on the others. Generally, the surfactant molecules possess an important property of reducing the interfacial tension. From the previous literatures, surfactants were used to prevent self-agglomeration of G by intercalation between G sheets [27-29]. Moreover, it was reported that surfactant can improve the interface property between electrode and electrolyte solution [30]. Also, it was well known that micelles are formed spontaneously in an aqueous solution at a sufficiently high concentration of surfactant. There are several applications that use micelles for electrode modification to improve the electrode surface properties [31, 32]. Accordingly, surfactant becomes a material of interest for developing of a new electrode platform for electrochemical sensor. Here, cetyl trimethylammonium

bromide (CTAB), a positively charged surfactant with quaternary ammonium group, is used together with G for electrode surface modification

In this study, the modified electrode was fabricated by electrochemical reduction of micellar GO on working electrode. This system based on electrochemically reduce micellar graphene oxide (ERMGO) modified electrode was applied for the simultaneous determination of CBF and CBZ in real agricultural products. The modified electrode preparation and optimization were systematically studied. In addition, this research also presents a comparison among our proposed electrode platform and the similar electrode systems (*e.g.* ERGO modified electrode) to show a superior performance. Overall, this modified electrode offers several advantages, such as fast and easy fabrication, high analytical performance, excellent electrochemical sensitivity and extremely low cost of materials. Indeed, this electrode platform will become an alternative approach for further development of electrochemical sensors in various applications.

1.2 Objectives

- To improve a hydrophobic property of graphene for suitable and efficient utilization for electrochemical detection in aqueous solution
- To develop electrochemical sensor based on electrochemically reduced micellar graphene oxide modified screen-printed carbon electrode
- To use modified electrode for applications of sensitive detection of carbofuran and carbendazim in agricultural products

1.3 Scope of the research

In this study, the electrochemical sensor based on electrochemically reduced micellar graphene oxide modified screen-printed carbon electrode was fabricated for the simultaneous determination of carbofuran and carbendazim. The applicable parameters concerning electrochemical sensitivity towards the analytes were investigated and optimized. Thence, modified electrode surface morphologies and properties were characterized by scanning electron microscopy, electrochemical impedance spectroscopy and contact angle measurement. Furthermore, the analytical

performances of modified electrode, including linear range, detection limit, were evaluated. Ultimately, under the optimal conditions, this proposed electrode system was applied for pesticide detection in real agriculture products.

CHAPTER II
THEORY

In this chapter, the basic principles and theory of electrochemical analysis are described. In the second part of this chapter, it focuses on carbon-based nanomaterials, especially graphene, graphene oxide and surfactant, used for electrode surface modification. Finally, the importance of the target analytes (carbofuran and carbendazim) are explained.

2.1 Electrochemical analysis

2.1.1 Fundamentals of electrochemistry [33]

Electrochemistry is a study about a relation between electrical energy and chemical reaction, and that reaction is called electrochemical reaction. The electrochemical reactions involve an electron transportation process of molecule or ion with changing its oxidation state. In fact, the principle of electrochemistry has been used for various applications, for example corrosion study, battery, fuel cell and electroanalytical sensor *etc*.

Electrochemical method, a class of techniques in electrochemical analysis, must be operated in an electrochemical cell with applying electrical signal towards the target analytes of interest, and measuring other electrical parameters, for example, current (amperes) or potential (volts). The electrochemical method can be divided into several categories depending on the measured parameters. For instance:

- Potentiometry; this technique is operated under static condition without current flowing, so the composition in electrochemical system is in equilibrium, and then potential is measured.
- Voltammetry; this technique is performed by varying applied potentials range, whereas a current signal is measured.
- Coulometry; this technique is operated by applying current or potential and measuring the amount of consumed or produced electricity (in coulomb)

In this work, we focused on a voltammetry technique. This technique has been generally used for electrochemical analysis application because of its powerful efficiency in analytical sensitivity and analytical performance.

2.1.2 Electrochemical cell

Basically, voltammetry must be operated with an electrochemical cell consisting of at least three main components: three electrodes, namely working electrode, reference electrode and counter (or auxiliary) electrode, electrolyte solution and external power supply. The working electrode is an electrode on which the electrochemical reaction of the analytes occurs. The reference electrode is used for measurement of the potential of working electrode without flowing any current through. Ultimately, counter electrode allows to pass current from working electrode to complete an electrical circuit. All the three electrodes are immersed into electrolyte solution containing target analytes. Meanwhile, the variation of potential between a pair of working-counter electrodes is controlled by external power supplied, known as potentiostat, and another function of potentiostat is to measure a current signal which gets along with potential change.

Figure 2.1 shows a conventional voltammetric cell. Three solid rods of electrode are immersed in an electrolyte solution; thus, this electrode system requires a large sample volume. Moreover, because of large instrumental components, this system is still non-portable. For the sake of convenience, the conventional electrode system is miniaturized into a smaller electrode system by using screen-printed electrode. Conductive ink, such as carbon ink or silver ink, are printed onto a substrate. Figure 2.2 shows a typical screen-printed carbon electrode on which working electrode and counter electrode are printed by carbon ink, and reference electrode is printed by silver ink. Instead of immersion of electrodes, the electrolyte solution containing analytes is readily dropped onto the electrode surface, covering three printed electrodes. The several advantages which this electrode offers over the conventional one are portable size, simple and rapid analysis and small sample requirement.

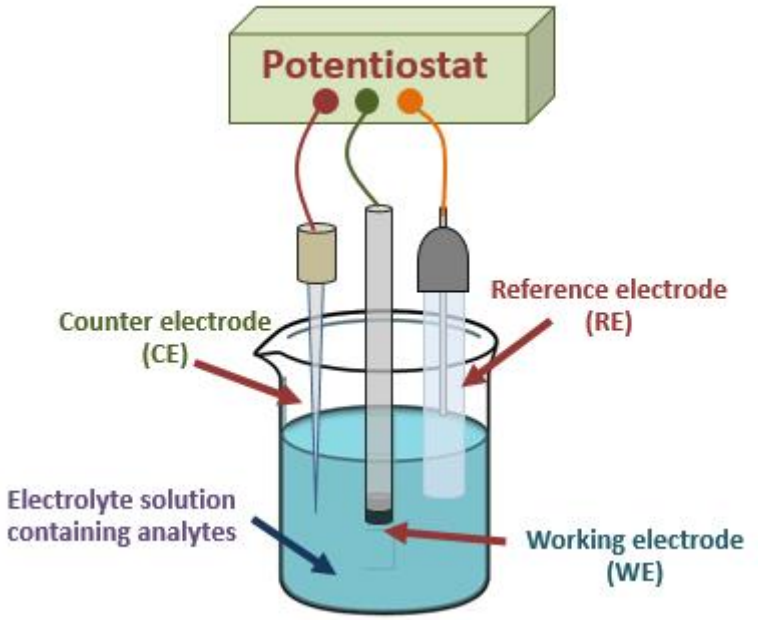

Figure 2.1 A conventional voltammetric electrochemical cell.

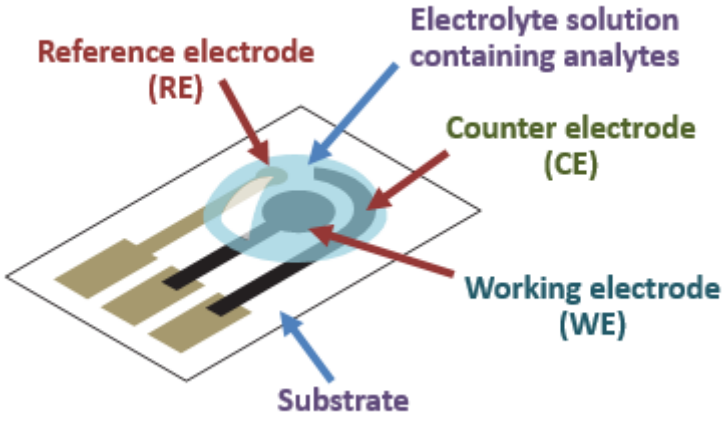

Figure 2.2 A screen-printed carbon electrode.

2.2.3 Electrode potential and Nernst equation

As long as potential is applied to the working electrode, a redox reaction of target analytes take place on the electrode surface. In the condition of very fast electron transfer and reversible process of the system, the current response is related to the concentration of the target analytes by Nernst equation as below:

$$E = E^0 + \frac{2.3RT}{nF} log \frac{C_o}{C_R}$$

Where E^0 = stand potential for the redox reaction, C_O = concentration of electroactive species in reduced form, C_R = concentration of electroactive species in oxidized form, R = the universal gas constant (K^{-1} mol^{-1}), T = Kelvin temperature, n = number of electrons transfer in the reaction, and F = the Faraday constant.

In an electrochemical cell, the current flowing in the system, which is caused by electrochemical reaction, can be divided into 2 types, faradaic current and non-faradaic current. The faradaic current can be generated by the oxidation or reduction reaction of the analytes on the electrode surface. On the other hand, non-faradaic current arises from a charge associated with movement of ion species or adsorption/desorption on the electrode-electrolyte solution interface, and non-faradaic current can also be called charging current. For the quantitative analysis, only faradaic current is considered because this current can indicate amount of redox reaction of the analytes on the electrode surface. The redox reaction of analytes is occurred by the excursion of analytes from bulk solution to electrode surface region with mass transfer process.

2.2.4 Mass transfer in electrolyte solution

Mass transfer is the movement of particles from one location in solution to another. Both analytes and electrolytes can be moved from the bulk solution to electrode surface under a condition of difference chemical or electrical potential at the two locations or from movement of a volume element in the solution. Mass transfer process can be divided into three types:

- Diffusion mass transfer; a movement of species under the influence of a gradient of chemical potential (*e.g.* concentration gradient)
- Migration mass transfer; a movement of charged substances under the inducement of an electrical field.
- Convection mass transfer; a movement from stirring or hydrodynamic transportation.

When three modes of mass transfer concur during analysis, the electrochemical system is much more complicated; therefore the system might frequently be designed

to avoid the contribution of one or more forms of mass transfer. For example, in the system of migration mass transfer, negatively charged and positively charged substances are enticed and repelled by same or opposite charge of applied potential surface; hence this system is unpredictable consequences of the migration current. Therefore, the effect of migration transfer might be reduced by addition of an inert electrolyte (a supporting electrolyte) at a much higher concentration than analyte species. Ultimately, the convection mass transfer can be avoided by the prevention of stirring or vibration of the solution in an electrochemical cell. Thus, mass transfer can be restricted to only diffusion mass transfer, called diffusion control, so the system is relatively much simpler to predict the phenomenon of diffusion pattern and the mathematical models.

2.2.5 Electrochemical methods

2.2.5.1 Potential step method under diffusion control

Figure 2.3a shows a diagram of the waveform applied in the basic potential step method. This kind of experiment can also be called chronoamperometry. A constant potential is stepped constantly from the point potential which redox reaction does not occur (none of faradaic process) (E_1) to the point potential which redox reaction occurs (E_2) monitored as a function of time. Figure 2.3b shows a curve i-t profile. At the beginning of potential stepping, both faradaic current and charging currents are generated because the potential is pulsed immediately. Later, the current in i-t profile decay exponentially with a progression of time. An effect of charging current decreases because there is no any movement of particles at the fixed potential. The system remains only diffusion mass transfer of electroactive species. Under the condition of diffusion control, faradaic current (i_d), which is due to electron transfer of the species and is only current component of interest, can be calculated by Cottrell equation:

$$i_d(t) = \frac{nFAD_o^{\frac{1}{2}}C_o}{\pi^{\frac{1}{2}}t^{\frac{1}{2}}}$$

Where $i_d(t)$ = the diffusion-limited current as a function of time (ampere), n = number of electrons involved in an electrode reaction, F = Faraday constant, A = area

of electrode surface (cm^2), D_o = diffusion coefficient (cm^2/s), C_o = bulk concentration of electroactive species (mol/cm^3), and t = time (s)

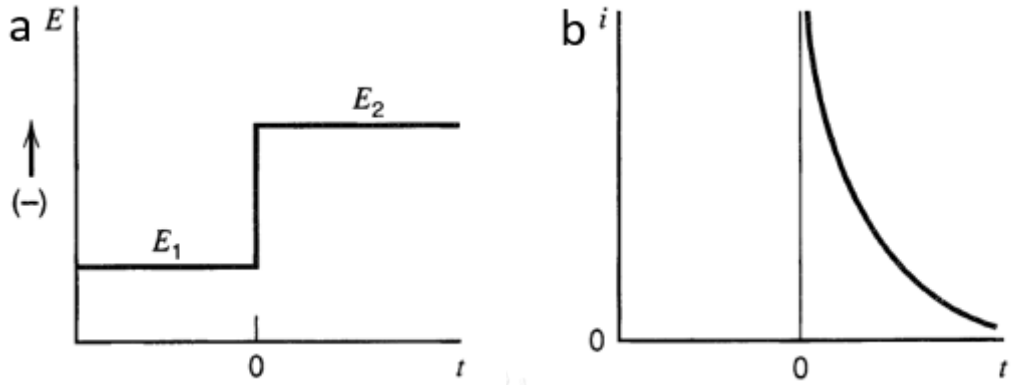

Figure 2.3 Applied potential waveform (a) Current flow vs. time (b).

2.2.5.2 Cyclic voltammetry (CV)

Cyclic voltammetry is a technique of the reversal experiment in linear scan voltammetry. The potential is swept linearly versus time in forward direction and switched direction of the scan to the opposite direction at a certain potential (E_λ) as shown in Figure 2.4a. The output from cyclic voltammetry experiment can be called cyclic voltammogram as shown in Figure 2.4b. The peaks of cyclic voltammogram indicate the electrochemical reaction occurring on the working electrode surface. The typical cyclic voltammogram displays two peaks belonging to oxidation and reduction reaction of electroactive species, and the peak can be called cathodic peak and anodic peak, respectively. Besides, the resulting currents are called peak current (i_p) which are obtained from the height of the peaks, and the corresponding peak potential (E_p) can be taken from the points of potential in which the peak currents are located. To sum up, the information in the voltammogram would exhibit four values of cathodic peak current (i_{pc}), anodic peak current (i_{pa}), cathodic peak potential (E_{pc}) and anodic peak potential (E_{pa}).

This technique has been widely used for obtaining qualitative information about electrochemical processes of target analytes, for example, a presence of intermediate in oxidation-reduction reactions and the reversibility of a reaction. CV can

also be used to determine the electron stoichiometry of a system, the diffusion coefficient of the analytes and the formal reduction potential *etc*.

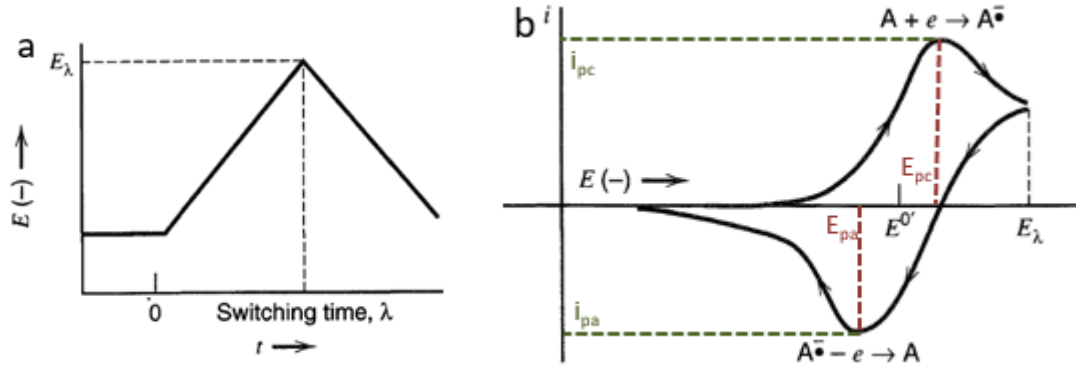

Figure 2.4 Applied potential waveform of cyclic voltammetry (a) cyclic voltammogram (b).

Considering about the redox reaction, the reversibility of a reaction can be distinguished with an experiment of cyclic voltammetry, and it can be separated into 3 types of systems.

1) Reversible system (or Nernstian system)

On the condition that the rate of electron transfer process is very rapid at the electrode surface so that it can maintain the concentration of the species at the electrode surface which is required by Nernst equation. The forward and reverse direction of redox reaction can totally occurs; therefore, the cyclic voltammogram displays two peaks of cathodic and anodic peak with symmetrical shapes. There are three defined characteristics for the reversible electrochemical reaction which we can consider whether the electrochemical behavior is reversible or not by interpretation of the information obtained from cyclic voltammogram.

- The difference between E_{pa} and E_{pc} (ΔE_p) is always close to 2.3RT/nF (or 59/n mV at 25°C).
- The ratio of the peak current, i_{pa}/i_{pc} is approximately equals to 1.
- The positions of peak potential are independent from a function of scan rate.

Interestingly, there is an equation showing relation between peak current as a function of several parameters, and the peak current can be calculated by this equation, called Randle-Sevcik equation as shown below:

$$i_p = 0.4463\left(\frac{F^3}{RT}\right)^{\frac{1}{2}} n^{\frac{3}{2}} A D_o^{\frac{1}{2}} C_o v^{\frac{1}{2}}$$

$$i_p = (2.69 \times 10^5) n^{\frac{3}{2}} A D_o^{\frac{1}{2}} C_o v^{\frac{1}{2}} \quad \textit{(at 25°C)}$$

Where i_p = peak current (ampere), n = number of electrons involved in an electrode reaction, F = Faradaic constant, A = electrode surface area (cm^2), D_o = diffusion coefficient (cm^2/s), C_o = bulk concentration of electroactive species (mol/cm^3), and $\boldsymbol{\nu}$ = scan rate (v/s).

2). Quasi-reversible and irreversible systems

Reversibility of the electroactive species depends on the relative values of electron transfer rate constant (k_0). Both irreversible and quasi-reversible behavior of the electroactive species shows that the electron transfer kinetics is limited. Providing the ratio of electron transfer rate constant and scan rate is sufficiently small that Nernstian concentration cannot be maintained, this system is called quasi-reversible. We can observe that a voltammogram of quasi-reversible system will display unequal peak heights of cathodic and anodic peak current, or the peak shape will distort with increasing scan rate as shown in Figure 2.5a and 2.5b, respectively. On the other hand, irreversible system can be caused by electron transfer rate constant is extremely small so that the redox reaction of the species occurs very slowly to be measured the current signal. For irreversible system, it can be verified by that the voltammogram exhibits either cathodic peak or anodic peak as shown in Figure 2.5c.

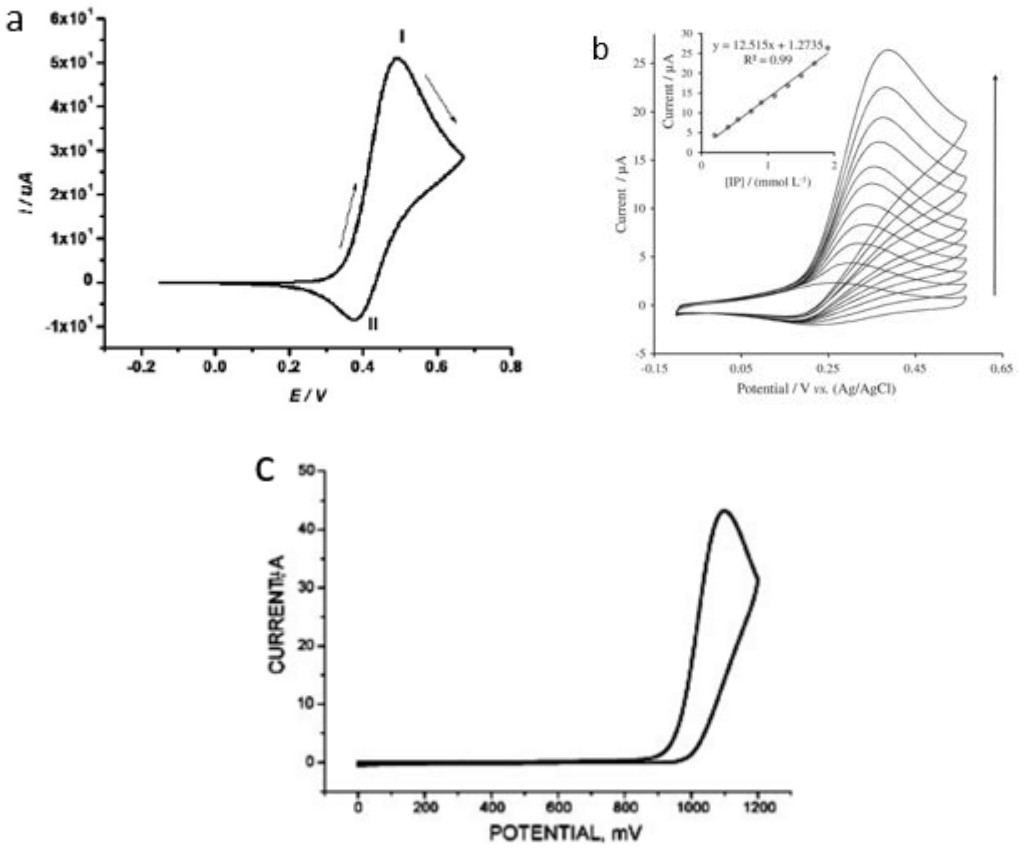

Figure 2.5 Cyclic voltammogram representing quasi-reversible system with unequal peak height of cathodic and anodic peaks [34] (a) quasi-reversible system with peak shape distortion with various scan rate [35] (b) irreversible with only anodic peak current [34] (c).

2.2.5.3 Square-wave voltammetry (SWV)

Square-wave voltammetry is one of pulse voltammetry techniques invented by Ramalet and Krause. SWV has been developed by a combination of the aspect from several pulse voltammetric methods. For example, the background subtraction and excellent sensitivity of differential pulse voltammetry (DPV), the demonstrative value of normal pulse voltammetry (NP) and the ability to directly study product of reverse pulse voltammetry (RP). Thus, this method has been widely used for trace quantitative analysis in a field of electrochemical sensor.

For SWV experiments, the potential waveform in SWV (Figure 2.6), displays that the potential is linearly swept along a progression of time at a working electrode surface. The additional functions were applied by bipolar square wave consisting of forward potential pulse and reverse potential pulse, deemed to be a cycle, and two current samples are taken twice per a cycle at the end of each pulse's lifetime (t_p). The forward current sample (i_f) represents in the same direction of staircase. On the contrary, the reverse current sample (i_r) is the opposite direction. Moreover, the differential current, which is always used as a diagnostic value, (Δi) can be calculated from subtraction of i_f and i_r. Thereby, in the single run of SWV, outputs will exhibit three information of current signals at the time, showing forward, reverse and differential current versus the applied potential, called square-wave voltammogram.

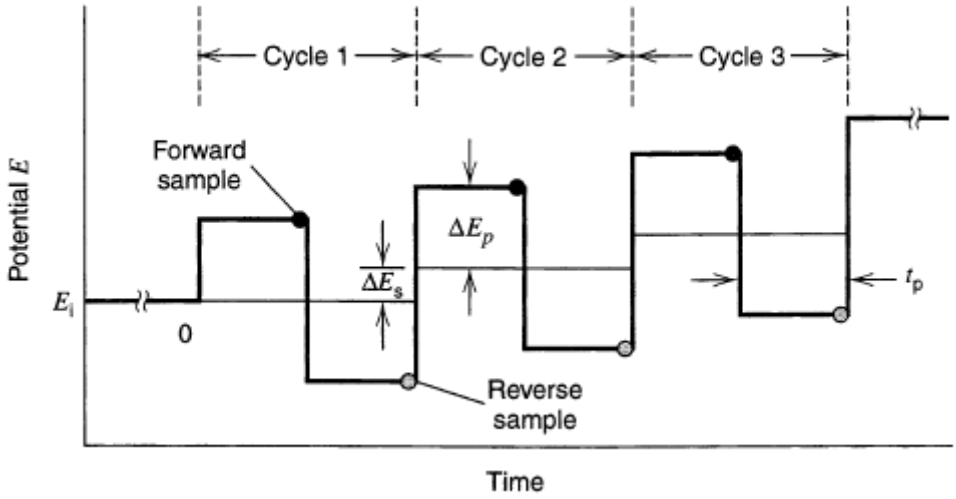

Figure 2.6 Waveform and sampling scheme of square-wave voltammetry in a plot of applied potential versus time.

According to SWV waveform, Figure 2.6 illustrates the important concerning parameters. Firstly, the square wave is characterized by a potential pulse height or pulse amplitude (ΔE_p) with holding pulse potential or pulse width (t_p), treading the staircase. In the meantime, the square wave is applied with the celerity of square wave frequency (f). The staircase shifts towards by ΔE_s at the beginning of each cycles, called a step potential. Ultimately, the scan begins at an initial potential (E_i) which can be applied to the system as desired.

The Figure 2.7 shows a dimensionless representation of the square-wave voltammogram that could be derived from an experiment like above explanation. As seen, the three information would be obtained from an experiment consisting of forward current (ψ_f), reverse current (ψ_r) and differential current ($\Delta\psi$) in the form of dimensionless current responses. Also, the forward and reverse currents have diagnostic value and resemblance of curve as same as cyclic voltammogram. On the other hand, the differential currents could be obtained from an absolute difference between forward and reverse currents, resembling differential pulse voltammogram.

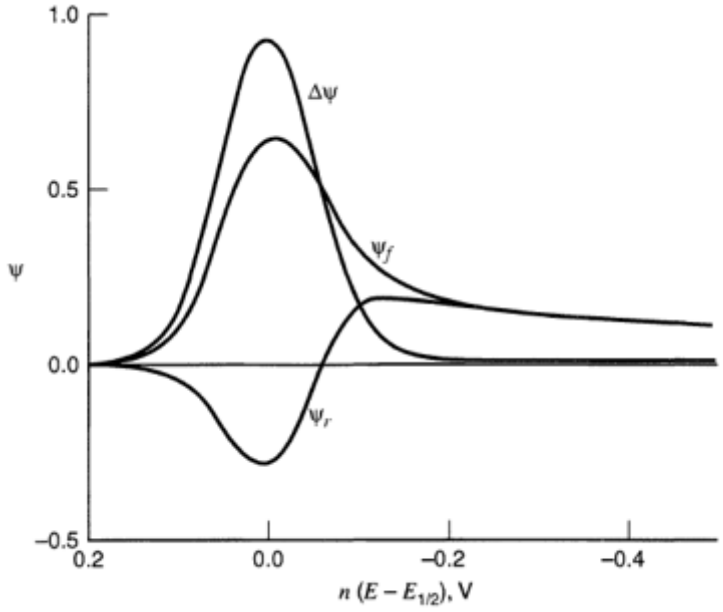

Figure 2.7 Square wave voltammograms showing forward currents (i_f), reverse currents (i_r) and differential currents (Δi) versus applied potentials.

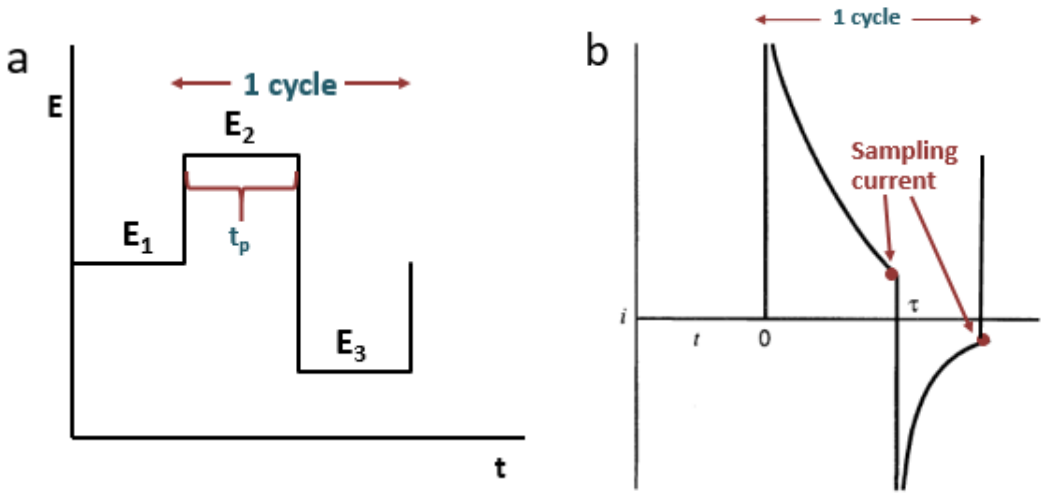

Figure 2.8 A cycle of square wave pulse (a) current response from a cycle of square wave pulse (b).

Considering a cycle of square wave as shown Figure 2.8a, the applied potential of forward pulse is raised up from E1 to E2 and held for the time of the pulse width (t_p). Thereupon, the applied potential is switched to reverse direction and also held at E3 for t_p. On the other word, in one cycle of the square wave appears to be a combination of two waveforms of chronoamperometry adjoining together. Thus, the output can be obtained as the construction between to current responses with the contrast direction of current signals. As seen in Figure 2.8b, the current samplings are based on i-e curves of chronoamperometry, so the current signal can be calculated by Cottrell equation model with the term of dimensionless parameters ($\Delta\psi_p$) as an equation below:

$$\Delta i_p = \frac{nFAD_o^{\frac{1}{2}}C_o}{\pi^{\frac{1}{2}}t_p^{\frac{1}{2}}}\Delta\psi_p$$

Where Δi_p = the actual peak current, n = number of electrons involved in an electrode reaction, F = the Faradaic constant, A = area of electrode surface (cm^2), D_o = diffusion coefficient (cm^2/s), C_o = bulk concentration of electroactive species (mol/cm^3), t = time (s) and $\Delta\psi_p$ is the dimensionless parameter which depends on n, ΔE_p and ΔE_s.

2.2.5.4 Electrochemical impedance spectroscopy (EIS) [36]

Electrochemical impedance spectroscopy (EIS) is an important electroanalytical techniques based on the measurement of the response in terms of the resultant ac voltage of circuit element to the applied currents. As long as a voltage signal of any frequency is applied, the impedance is a function of the frequency, and an impedance spectrum is a representative of the impedance of a circuit element as a function of frequency. Therefore, impedance can be used to measure the ability of a circuit resisting the flow of alternating electrical current.

The chart output obtained from EIS experiment is called Nyquist plot which consists of semicircular region on the axis followed by a straight line as shown in Figure 2.9. The semicircular portion can be created at higher frequencies, and the straight line can be observed at lower frequencies. The Nyquist plot informs an important information about electrified surface and electron transfer reaction. The semicircular portion involves to the electron-transfer-limited process (charge transfer). On the other hand, the straight line is characteristic of mass transfer process (diffusion limited process). Therefore, impedance spectrum can be used to study the kinetic of electron transfer process and diffusion-limited process. The diameter of the semicircular from Nyquist plot directly corresponds to the electron transfer resistance (R_{ct}), and it can be calculated by an equation below:

$$R_{ct} = \frac{RT}{Fi_0}$$

Where R_{ct} = electron transfer resistance, R = gas constant, T= temperature, F = Faraday constant and i_0 = the exchange current. Because we have known the relation between the exchange current (i_0) and rate constant (k^0) which is

$$i_0 = FAk^0C$$

Therefore, we will obtain the relation between the electron transfer resistance and rate constant, which, in this case, refers to rate of electron transfer process as an equation below:

$$k^0 = \frac{RT}{R_{ct}FAC}$$

According to this equation, the electron transfer rate is inversely proportional to the resistance of electron transfer. If the kinetic of electron transfer process is very fast, the resistance of electron transfer remains infinitesimal; thus, the impedance will be only linear part. On the contrary, if the kinetic of electron transfer process is slow, the semicircular portion will be existed.

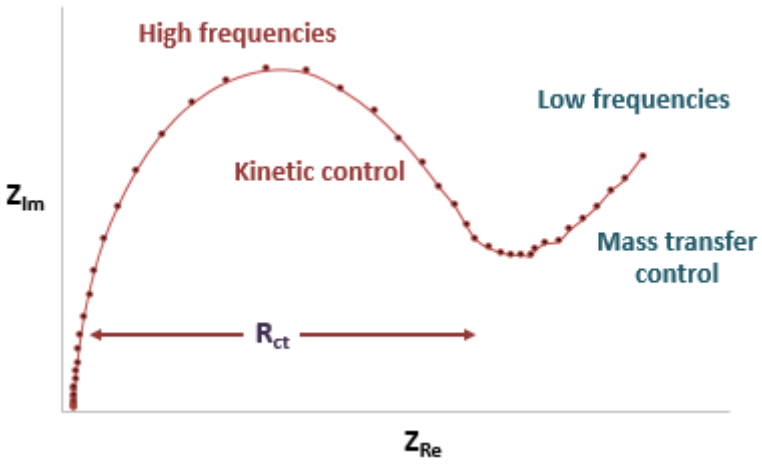

Figure 2.9 A typical electrochemical impedance spectrum in term of Nyquist plot.

2.2 Nanomaterials

2.2.1 Introduction

Nanomaterials are materials described as a single unit particle which is one or more external dimensions is sized in nanoscopic scale ranging from 1 to 100 nm. Because of their small scale particles, nanoparticles would be materials which possess a property of large surface area. Therefore, nanoparticles are suitable to be used in the applications which is required the high surface area. Furthermore, on the condition that reduces a size of particles into a nanoscale, their properties could be outright changed, such as magnetic, optical and electronic properties.

2.2.2 Carbon-based nanomaterials

In this study, carbon-based nanomaterials are focused because they have received the intense attention in the scientific researches. Moreover, carbon-based nanomaterials also possess several unique combination of chemical and physical properties [37] (*e.g.* high specific surface area, thermal and electrical conductivity,

mechanical strength and optical properties). Therefore, they are promising to be used for electrode surface modification.

The first discovery of carbon-based material is fullerene in 1985. Fullerene is one of the carbon family which is allotropic carbon structure in the form of a hollow sphere or tube. A type of allotrope which is made up from carbon atoms joined in the pattern of ball is generally called Buckminster fullerene. The molecules of Buckminster fullerene are spherical and are also known as buckyballs, and there are several formula, such as c_{28}, c_{36}, c_{50}, C_{60} and C_{70} *etc.* as shown in Figure 2.10. Due to its property of large surface area and fairly good electrical conductivity, fullerenes have attracted the considerable attention for electrochemical analysis field [13].

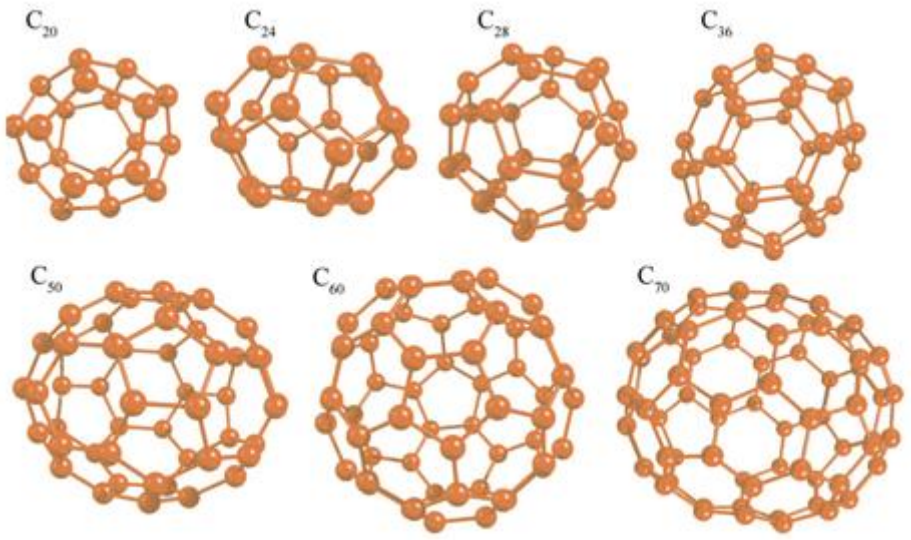

Figure 2.10 Structures of Buckminster fullerene molecules with various formula.

Carbon nanotubes (CNTs), an allotrope of carbon with cylindrical nanostructure, were discovered in 1991. Carbon nanotube are also a member of fullerene carbon family constructed from hexagonal carbon structures. There cylindrical carbon molecules have many unique properties, such as mechanical, electrical and electrochemical properties. Therefore, they were attracted more research interest than fullerenes for being used for electrode modification because CNTs offer several advantages, such as high electrical conductivity, large surface area, an ability of establish **π**-**π** interaction and excellent thermal, chemical and mechanical

stability. Moreover, CNTs can be used for covalent and non-covalent functionalization on their surface; therefore, CNTs were popularly used to be electrode modification for enzyme-immobilizing biosensor.

Besides, CNTs, as shown in Figure 2.11, can occur as multiple concentric cylinders of carbon atoms coupled together with Van Der Waals interaction, called multi-walled carbon nanotubes (MWCNTs). Since MWCNTs was discovery in 2003, MWCNTs became a promising material. Owing to their advantages over single-walled CNTs, they have attracted more research interest, and the applications of MWCNTs in electrochemical analysis research have highly increased in recent years.

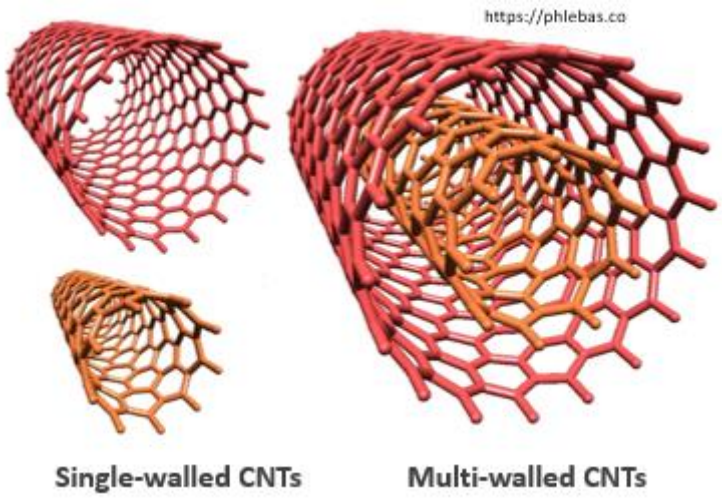

Figure 2.11 Structures of single-walled and multi-walled carbon nanotubes.

Graphene is a new allotrope of carbon family which is, basically, in a form of single atomic layer sheet of graphite packed together with tightly bonded sp^2-carbon hexagonal lattice structure as shown in Figure 2.12. Since the first observation and characterization of mechanical exfoliation of graphene in 2004 [38], G has become considerably growth of research in scientific and engineering communities because graphene structure has shown several extraordinary properties (*e.g.* excellent electronic, optical and mechanical properties, large surface area, excellent electrical and thermal conductivity *etc.*). Due to its excellent properties, graphene has inspired many applications in a variety of fields, including clean energy devices, electronics, catalysis, biomedicine and sensors.

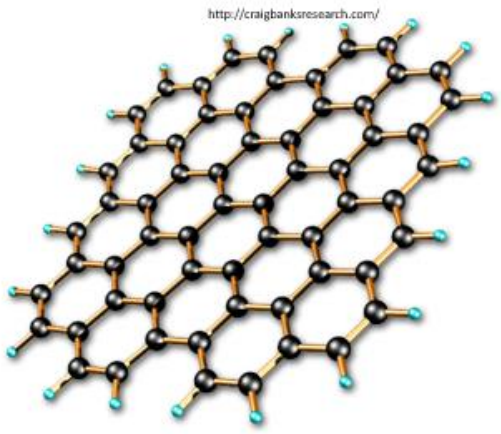

Figure 2.12 Structure of graphene.

Lately, some researches has reported that the use of pristine or modified graphene as electrode modification material provides higher efficiency than other allotropes of carbon-based nanomaterials. Moreover, due to their similar chemical structures [18], graphene is considered as a parent form of graphite, fullerene and CNT. For example, graphene is simply an isolated layer of graphite, or single-walled CNTs are made up from a graphene sheet rolling in a shape of a cylinder, or Buckminster fullerene can be considered as a graphene sheet in a form of sphere, so the advantages of fullerene and CNT undoubtedly belong to graphene as well. Nowadays, in analytical analysis, graphene has become more interesting material than other carbon allotropes for the reasons:

- Due to a unique nanosheet morphology, graphene has a very large specific surface area which a value of surface area is theoretically evaluated to be 2,630 m^2/g [39], suggesting that graphene has an immense surface area for a high adsorption capacity. For fullerene and CNT, the inner walls are probably unavailable for the absorption on the surface because of steric hindrance.
- Graphene can be synthesized from a very common and cheap material by simple chemical methods without any special device [40]. In other words, graphene can be readily obtained by using simple chemical laboratories, so it can be applied for extensive application and large scale synthesis.

- A synthesis procedure of CNTs must be proceeded along with metal catalysts, so there is unavoidably contain residual metallic impurities which is difficult to purify or remove [41]. However, graphene can be synthesized from graphite without using metal catalysts, so it is easier for purification to obtain a clean product.
- Graphene sheet are relatively flexible and soft, so it can be functionalized on the surface more easily than CNTs fullerenes concerning steric hindrance effect [42].

From the above reasons, graphene has adequately good properties to replace CNT and fullerene for using as an electrode modification material. In this work, we focus on using graphene along with other material for fabrication of a novel graphene-based nanocomposite in order to improve electrode surface properties in electrochemical sensor.

2.2.3 Synthesis and characterization of graphene

The first successful approach to produce single-layer or few-layer graphene was obtained from mechanical exfoliation of graphite by using Scotch tape [38]. This method can produce high-quality product, but the yield is extremely low, and the producing process is uncontrollable.

Afterwards, scientists attempted to develop the methods for synthesizing a large quantity of graphene by following methods: chemical-vapor deposition (CVD), epitaxial growth, arc discharge and substrate gas-phase synthesis [43, 44]. However, these methods still have some drawbacks as follows:

- The process requires high-quality substrate, high temperature and precise temperature control, thus it is unsuitable for large-scale production.
- In the process of graphene synthesis, a large amount of metal catalyst was used, so it may left some impurities in graphene product. The purity of the graphene may affect to the subsequent applications.

- Due to the very strong hydrophobic property of as-prepared graphene, graphene tend to re-stack or agglomerate into graphite. Many unique properties of graphene are concerned only with individual sheet. Thus, providing graphene aggregates in the solution, it causes decreased specific area and electrical conductivity of graphene.

As above mention, chemical synthesis of graphene has been subsequently developed, and it shows to be one of the most efficient methods because of its advantages, such as low cost, large-scale production [40]. As the chemical synthesis of graphene, graphite is used for a starting material, and oxidation reaction of graphite is occurred to be graphene oxide as an intermediate. Afterwards, exfoliation of individual graphene single sheets can be carried out by ultrasonication. Finally, the graphene oxide can be converted to graphene by a reduction reaction, called chemically-converted graphene (CCG) as shown in Figure 2.13.

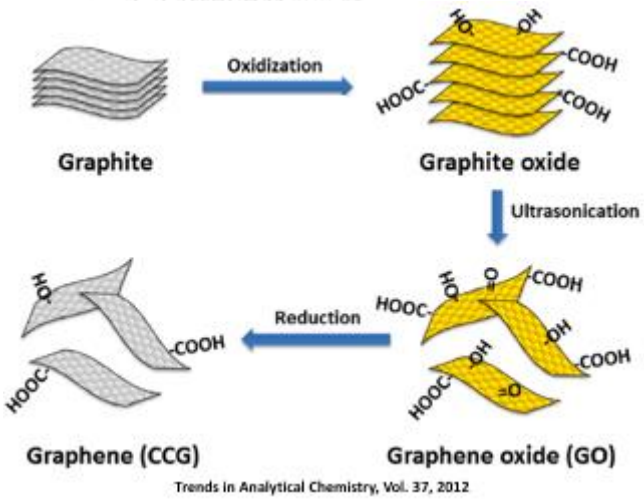

Figure 2.13 The chemical synthesis route to graphene from graphite as starting material[37].

In the step of an oxidation reaction of graphite, highly strong oxidizing agents (oxidizers), such as a mixture of sulfuric acid and potassium permanganate solution ($H_2SO_4/KMnO_4$), were used for oxidizing because graphite is often considered as an inert compound. Oxidizer works by reacting with graphite and removing electron in the chemical reaction. Then, graphite which is oxidized would be converted to graphene

oxide, a non-conductive graphene derivative. Graphene oxide is a compound made up from graphene sheets with a lot of decorations of oxygen functional groups. As shown in Figure 2.14, the structure of graphene oxide and graphene are very similar, but the properties are totally different. Considering polarity of graphene oxide, it has a property of hydrophilicity. As this reason, graphene oxide could be dispersed very well in aqueous solution and it possessed only small interaction with themselves via hydrogen bond. However, oxygen functionalities on the graphene surface would disrupt the sp^2 bonding network, meaning that graphene oxide is often described as an electrical insulator.

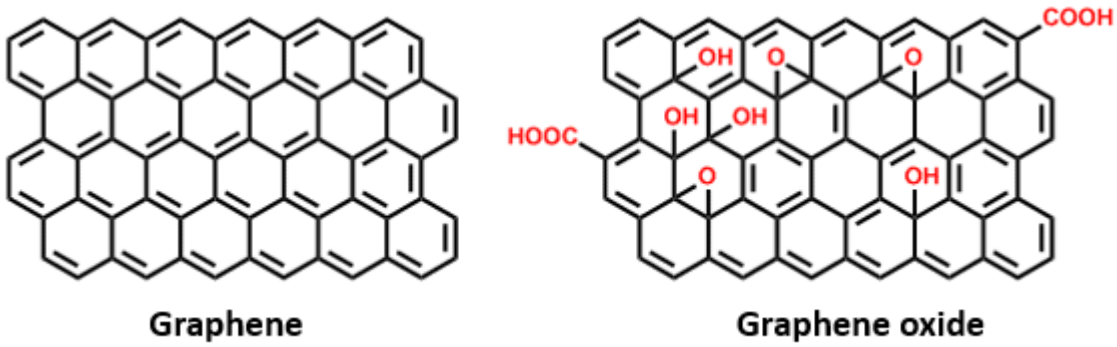

Figure 2.14 Structures of graphene and graphene oxide [45].

Thereupon, the process of turning graphene oxide to graphene can be approached by a reduction reaction. In the reduction process, oxygen functionalities would be eliminated, and then the structure remains a bare carbon structure of pristine graphene, also called reduced graphene oxide (RGO). In the previous researches [19], there are several ways of the reduction of graphene oxide. These methods have both advantages and disadvantages, and the selection of the method depends upon a preferable application. So far, scientists have invented the process to generate reduced graphene oxide from graphene by:

- Graphene oxide can be reduced by strong reducing agents through chemical reaction. At the first discovery, hydrazine was frequently used as a reductant [46]. Nevertheless, other environmentally-friendly and low-toxicity reducing agents have been used in place, for example, ascorbic acid

[47], $NaBH_4$ [48] or iron powder [49] *etc.*). Moreover, reducing graphene oxide by chemical reaction are very scalable method, but this method would produce relatively poor-yield products because of impurities of reducing agent.

- Graphene oxide can be converted to be graphene by thermal reduction which can be divided into 2 types: thermal annealing [50, 51] and microwave [52] and photo reduction [53]. In this method, very high temperature (≥500° C) is used for thermally reducing graphene oxide. This method can create reduced graphene oxide which has a very high surface area. Unfortunately, with very high temperature, the heating process can damage graphene structure during building up pressure and releasing of carbon dioxide from graphene oxide structure [24].
- Graphene oxide can also be reduced by electrochemical method, called electrochemically reduced graphene oxide (ERGO). The electrochemical reduction of graphene oxide is a method that has been shown to produce a very high quality and purity of products because ERGO can be obtained without hazardous chemicals [23]. In the recent researches, ERGO shows a very high carbon to oxygen ratio and electronic conductivity [54]. The only disadvantage is that this method can create a small yield of reduced graphene.

In this research, we are interesting in ERGO due to its exceptional properties, such as possession of large surface area, very high electrical conductivity and being a good electrocatalytic activity. Therefore, ERGO would be used as one of the materials for electrode surface modification in electrochemical sensor.

2.3 Surfactant

Surfactants are the surface-active compounds. Generally, surfactant can act as detergent, wetting agent, emulsifier, foaming agent and dispersant. The surfactant molecules possess an important property of lowering the surface tension (or the interfacial tension) between two phases. Their structure are amphiphilic molecules

consisting of hydrophilic head on one side and long chain hydrophobic tail on the others (as shown in Figure 2.15a), so their molecules contain both water soluble and water insoluble (or oil soluble) parts. As long as surfactants are added into the water, their molecules will align along the air-water or oil-water interfaces which hydrophilic part is in water phase and hydrophobic part is in air or oil (as shown in Figure 2.15b). On the condition that surfactants are added continuously so that the concentration of surfactants is higher than a given point, called the critical micelle concentration (CMC), the surfactant molecules will form micelles where hydrophilic heads form self-assembly structures to contact aqueous solution and hydrophobic tail sequesters inward the center (as shown in Figure 2.15c)

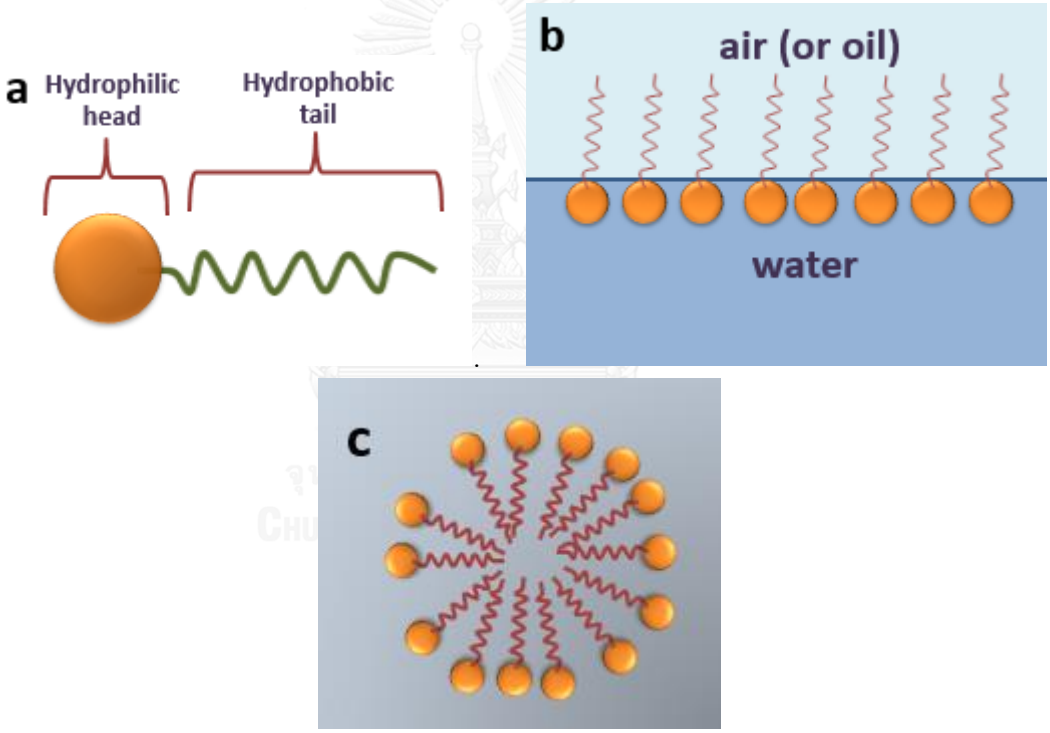

Figure 2.15 Structure of amphiphilic molecule (a) amphiphilic molecule on air-water interfaces (b) micelle (c).

The critical micelle concentration (CMC) is defined as the concentration above which any added surfactant molecules appear as micelle aggregation. At the low concentration of surfactant, their molecules will arrange themselves on the surface. When more surfactant is added, the surface tension of the solution start to rapidly decrease because more surfactant molecule will be on the surface. With high enough

concentration of surfactants (the concentration of surfactants surpassing CMC), the surface become saturated. The addition of the surfactant molecules cause formation of micelles. A graph of surface tension versus logarithm of surfactant concentration is shown in Figure 2.16. Three different phases can be identified:

- Phase 1: At very low concentration of surfactant, surface tension is slightly changed.
- Phase 2: With the addition of surfactant, surface tension drastically decreases.
- Phase 3: At CMC point, surfactant orientation at the surface becomes saturated, and the addition of more surfactant no longer affects to the surface tension. Besides, the excess amount of surfactant molecules spontaneously forms micelles.

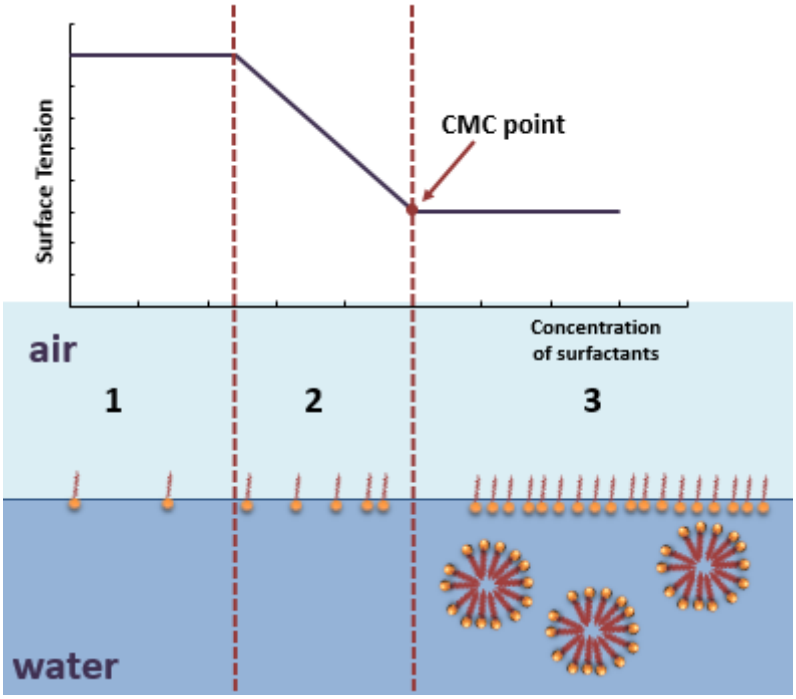

Figure 2.16 Surface tension between water and air interface against the surfactant concentration.

Based on the types of hydrophilic heads, surfactants can be classified into 4 groups:

- Anionic surfactant; this type of surfactants possesses negatively charged hydrophilic group. They are widely used this type for laundering, dishwashing liquid and shampoo. They are particularly good at keeping the dirt, once dislodged, away from fabric.

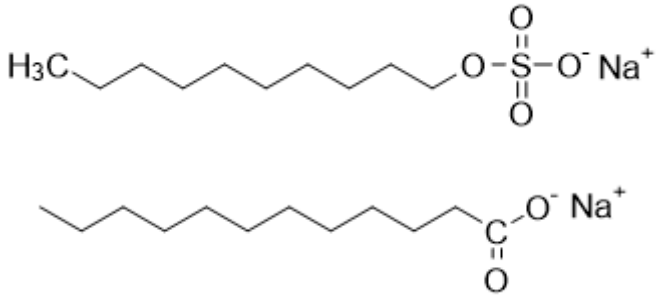

Figure 2.17 Examples of anionic surfactant.

- Cationic surfactant; for structure of cationic surfactants, the hydrophilic head has positively charged. This type of surfactants is often used for a specific purpose.

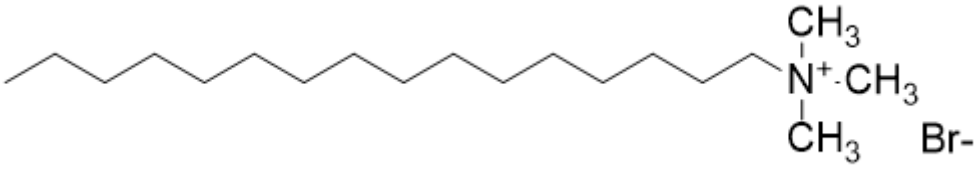

Figure 2.18 An example of cationic surfactant.

- Non-ionic surfactant; this surfactant do not show any electrical charge. An important advantage of this type of surfactant is that they do not interact with calcium or magnesium ions in hard water.

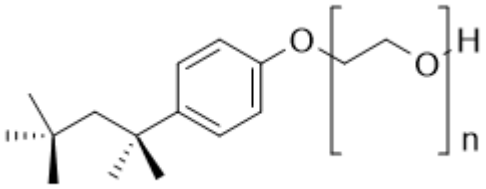

Figure 2.19 An example of non-ionic surfactant.

- Amphoteric surfactant; amphoteric (or zwitterionic) surfactant has hydrophilic head containing both a positive and negative charge. Amphoteric surfactants are very mild, they are often used in shampoo and other cosmetic because of their pH balanced property.

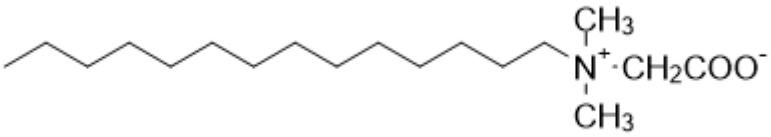

Figure 2.20 An example of amphoteric surfactant.

2.4 Target analytes

2.4.1 Carbofuran

Carbonfuran (CBF) is known as the most hazardous carbamate insecticide because of its high insecticidal activity. This type of insecticide is known under the trade names of Furadan. It is used to control pests in crop fields, such as potatoe, corn, soy bean. It is broad spectrum pesticide which has an ability of extermination of insects, mites and nematodes. Carbofuran can be toxic by inhalation and ingestion, and it can easily be taken through dermal absorption. Due to its dangerous property, carbofuran is banned in many countries, for example, Canada, the European Union and The United states of America [4].

In this research, there are some useful physical properties for the experiment as follows:

- Appearance: Carbofuran is an odorless, white crystalline solid.
- Chemical Name: 2,3-dihydro-2,2-dimethylbenzofuran-7-yl methyl carbamate
- Molecular weight: 221.25 g mol^{-1}
- Water solubility: 320 mg L^{-1}

- Solubility in other solvents: acetone, acetonitrile, benzene, cyclohexane and ethanol

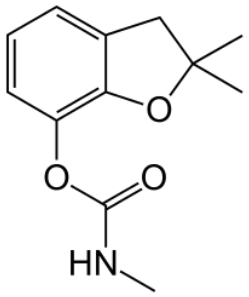

Figure 2.21 Chemical structure of carbofuran.

Numerous conventional analytical methods, such as capillary electrophoresis [55], gas chromatography [56], high-performance liquid chromatography [57], mass spectroscopy [58] and a rapid magnetic particle-based ELISA [59] technique had been employed for carbofuran detection. However, these techniques requires long analysis time, expensive instrument and using toxic reagents.

In the recent years, carbufuran has been developed to be detect by electrochemical analysis. Unfortunately, it has no property of electroactive species, so it cannot be detected by electrochemical method. Nevertheless, the development of electrochemical biosensor has been accomplished. Carbofuran can be effectively determined by biosensor [60] because it offers several advantages, such as high specificity and high sensitivity for real-time analysis in complex mixtures and simple operation without the need of sample pretreatment. Nonetheless, enzyme immobilized on sensor always need special care in case of temperature, pH, storage and enzyme activity, making these systems less robust and difficult to deal with. Therefore, considerable attention will focus on non-enzymatic system to avoid these drawbacks of the enzymatic system.

Because of non-electroactive property of carbofuran (Equation 2.1), it cannot be directly detected by electrochemical method which is based on electrochemical stimulation. From the previous literatures [61], it was reported that carbamate pesticides can produce electroactive phenol derivatives through a process of alkaline

hydrolysis at high temperature. As it is, CBF can be hydrolyzed to be CBF phenol (equation 2.2) in the alkalescent aqueous solution. Interestingly, the factors influencing on the alkaline hydrolysis of CBF was investigated and reported that the optimal condition for CBF hydrolysis is a hydrolytic temperature of 75°C and a heating time of 3 minutes [62]. Thereby, CBF can be indirectly determined by electrochemical detection with CBF phenol (equation 2.3).

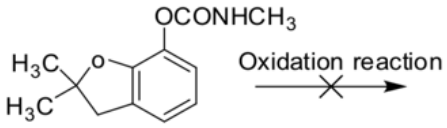

Equation 2.1 Non-electroactive CBF.

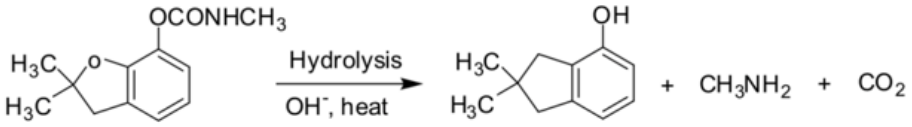

Equation 2.2 Hydrolysis of CBF.

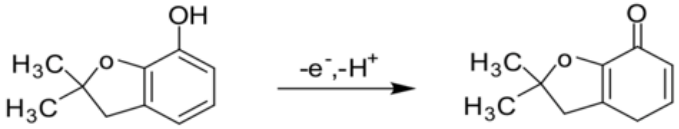

Equation 2.3 Oxidation reaction of CBF phenol.

2.4.2 Carbendazim

Carbendazim (CBZ), a benzimidazole based fungicide, is extensively used for wild range of plant disease control in cereals, fruits, including citrus, banana, strawberry, pineapple. It is considered as a highly toxic chemical because carbendazim possesses long degradation time due to its unbreakable chemical structure. Besides, some previous researches revealed that carbendazim is a carcinogenic substance causing chronic and acute disease. Carbendazim can access to human bodies by inhalation, ingestion and dermal absorption [2].

In this research, there are some useful physical properties for the experiment as a table below:

- Appearance: Carbendazim is light grey powder.
- Chemical Name: Methyl-2-benzimidazole carbamate
- Molecular weight: 191.19 g mol^{-1}
- Water solubility: 8 mg L^{-1}
- Solubility in other solvents: acetone, ethanol and chloroform

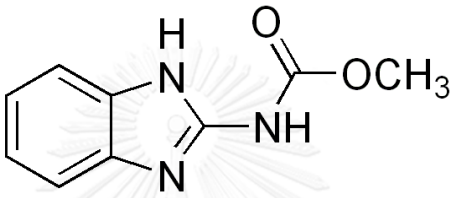

Figure 2.22 Chemical structure of carbendazim.

There are several conventional analytical methods commonly used for carbendazim detection, for example, high-performance liquid chromatography [9], mass spectroscopy [10], UV-vis and fluorescence spectroscopies [63]. Likewise, these techniques are not suitable for real-time detection, and they require complicated pretreatment, well-trained operator and time-consuming detection process. To overcome these disadvantages, electrochemical detection technique has been developed.

Furthermore, carbendazim is an electroactive species, so it can be directly detected by electrochemical method as shown in Equation 2.4.

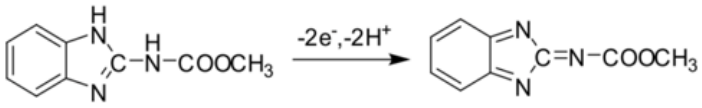

Equation 2.4 Oxidation reaction of CBZ.

2.4.3 Maximum Residue Limits (MRLs)

Maximum residue limit (MRL) database shows the maximum acceptable levels of pesticide and veterinary drugs in food and agricultural products in the United States

and 70 other countries, Including the European Union and the Codex Alimentarius Commission. The pesticide levels should not be left over in the foods listed more than the MRL (in mg/kg) of the pesticide residues (defined in each individual case in the definition of residue) at (a) the point of entry into a country or (b) at the point of entry into trade channel within a country.

From World Health Organization (WHO), the Codex Committee on Pesticide Residues stipulates regulation of MRLs for the maximum acceptable levels of carbofuran and carbendazim in agricultural products (soy bean, rice and tomatoe) as follows [64]:

Products/Pesticide	Carbofuran (mg/kg)	Carbendazim (mg/kg)
Soy beans	0.2	0.2
Rice	0.2	2.0
Tomatoes	0.1	0.5

CHAPTER III

EXPERIMENTAL

This chapter provides the details of chemicals and materials, apparatus, solution preparation, electrochemical detection and sample preparation procedure.

3.1 Chemicals and materials

- Graphene oxide (GO) (XF Nano, Inc., Nanjing, China)
- Cetyltrimethylammonium bromide (CTAB) (Sigma-Aldrich, St. Louis, MO, USA)
- Potassium dihydrogen phosphate (KH_2PO_4) (Sigma-Aldrich, St. Louis, MO, USA)
- Disodium hydrogen phosphate (Na_2HPO_4) (Sigma-Aldrich, St. Louis, MO, USA)
- Carbon graphene ink (Gwent group, Torfaen, United Kingdom)
- Silver/silver chloride ink (Gwent group, Torfaen, United Kingdom)

3.2 Apparatus

- The electrochemical measurements using square-wave voltammetry (SWV) and cyclic voltammetry (CV) were performed on a 910 PSTAT mini (Metrohm Siam Company Ltd.). SWV measurements of CBF and CBZ were carried out using an applied potential ranging from 0 to 1.0 V with the optimal parameters including a step potential of 10 mV, an amplitude of 20 mV and a frequency of 10 Hz.
- A three-electrode configuration of screen-printed carbon electrode with 4 mm of working electrode diameter was fabricated and used in this work.
- Electrochemical impedance spectroscopy (EIS) was performed on μAUTOLAB type III potentiostat (Metrohm Siam Company Ltd.) using a solution of 0.5 M KCl containing 1 mM $[Fe(CN)_6]^{3-/4-}$ with a frequency range of 0.1-10^{-5} Hz and an amplitude of 0.01 V.A.

- JSM-6400 field emission scanning electron microscope (Japan Electron Optics Laboratory Co., Ltd., Japan) was used for electrode surface morphology characterization.
- Contact angle measurement was performed on a 200-k1 goniometer (Rame-hart Instrument Co.).
- Block screen (Chaiyaboon Co., Bangkok, Thailand)

3.3 Fabrication of screen-printed carbon electrode

A three-electrode configuration of screen-printed carbon electrode pattern was designed by Adobe Illustrator. The electrodes were prepared by using an in-house screen-printing procedure as shown in Figure 3.1. At the beginning, silver/silver chloride was screened on PVC substrate as a reference electrode (RE) and a conducting pad, and then heated up at 55°C until the ink was dried out. Afterwards, carbon graphene ink was screened over as a working electrode (WE) and a counter electrode (CE), and heated up at 55°C till the ink was dried out.

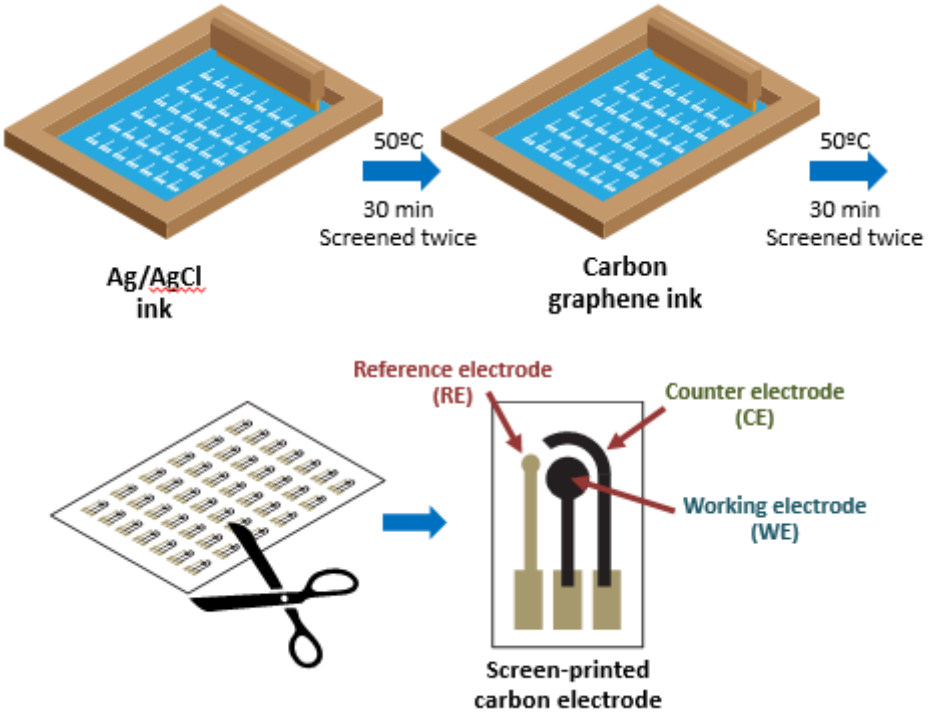

Figure 3.1 A fabrication scheme of screen-printed carbon electrode and the configuration of three-electrode system.

3.4 Preparation of solution

All aqueous solutions were prepared in Milli-Q water (12.8 MΩ cm).

3.4.1 Preparation of 0.1 M phosphate buffer solution pH 7.0 (PB solution)

1.4051 g of potassium dihydrogen phosphate (KH_2PO_4) and 2.0833 g of disodium hydrogen phosphate were dissolved in 250 mL of Milli-Q water.

3.4.2 Preparation of 1.6 mg mL^{-1} graphene oxide solution

1.6 mg of graphene oxide (GO) was dispersed in 1 mL of water with an ultrasonicator for 2 hours.

3.4.3 Preparation of 0.2 %w/v cetyltrimethylammonium bromide (CTAB) solution

0.02 g of CTAB was dissolved in 10 mL of water.

3.4.4 Preparation of graphene solution in phosphate buffer solution for electrode modification (GO solution)

The dispersed 1.6 mg mL^{-1} GO solution (from 3.4.2) was mixed with 0.1 M PB solution pH 7 at the ratio of 1:1, denoted as a GO solution.

3.4.5 Preparation of micellar graphene oxide solution in phosphate buffer solution for electrode modification (MGO solution)

The dispersed 1.6 mg mL^{-1} GO solution (from 3.4.2) was mixed with 0.1 M phosphate buffer solution pH 7.0 and 0.2 %w/v CTAB solution (from 3.4.3) at a volume ratio of 10:9:1, denoted as MGO solution.

3.5 Fabrication of modified electrode

3.5.1 Fabrication of electrochemically reduced graphene oxide modified electrode

100 µL of GO solution was dropped onto a SPCE, covering over 3 electrodes. Cyclic voltammetry was performed from -0.5 to -1.7 V (vs Ag/AgCl) at a scan rate of 100 mV s^{-1} for 10 cycles. Eventually, reduced graphene oxide was deposited on the working electrode surface. This modified electrode model is called ERGO modified electrode.

3.5.2 Fabrication of electrochemically reduced micellar graphene oxide modified electrode

100 µL of MGO solution was dropped onto a SPCE. Then, the reducing process was carried out by cyclic voltammetry in a potential range from -0.5 to -1.5 V (vs Ag/AgCl) at a scan rate of 100 mV s^{-1} for 10 cycles. Finally, reduced micellar graphene oxide are deposited onto the working electrode surface. This modified electrode model is denoted as ERMGO modified electrode.

3.5.3 Optimization of electrode modification

The important parameters influencing on the electrochemical response, including CTAB concentration, GO concentration, scan rate and number of scans, were optimized. The selected conditions were obtained by compromising between the highest peak current signal and the well-defined peak shape.

3.5.3.1 Effect of GO concentration

Effect of GO concentration was investigated by dispersing 0.5, 0.6, 0.7, 0.8, 0.9 and 1.0 mg mL^{-1} GO for preparation of MGO solution. Afterwards, Electrochemical reduction of MGO solution onto working electrode surface will be performed by cyclic voltammetry in a potential range from -0.5 to -1.5 V (vs Ag/AgCl) at a scan rate of 100 mV s^{-1} for 10 cycles.

3.5.3.2 Effect of CTAB concentration

Effect of CTAB concentration was studied by preparing 0.0025, 0.005, 0.010, 0.015, 0.020 %w/v and absence of CTAB in 0.8 mg mL^{-1} GO solution. Then, Electrochemical reduction of MGO solution onto working electrode surface was performed by cyclic voltammetry in a potential range from -0.5 to -1.5 V (vs Ag/AgCl) at a scan rate of 100 mV s^{-1} for 10 cycles.

3.5.3.3 Effect of scan rate

Effect of scan rate was investigated by cyclic voltammetry with various scan rates of 50, 100, 150 and 200 mV s^{-1} for 10 cycles during electrochemical reduction of MGO solution.

3.5.3.4 Effect of number of scans

Effect of number of scans was studied by using cyclic voltammetry with different numbers of scan of 5, 6, 7, 8, 9 and 10 cycles with scan rate of 100 mV s^{-1} during electrochemical reduction of MGO solution.

3.6 Characterization of modified electrode

3.6.1 Surface morphology characterization

The surface morphologies of unmodified electrode, ERGO modified electrode and ERMGO modified electrode were characterized by scanning electron microscopy (SEM) with the magnification of 1000x

3.6.2 Contact angle measurement

Hydrophobic and hydrophilic properties of unmodified electrode, ERGO modified electrode and ERMGO modified electrode were characterized by contact angle (CA) measurement.

3.6.3 Electrochemical characterization

For electrochemical characterization of modified electrode, unmodified electrode, ERGO modified electrode and ERMGO modified electrode were used by

using cyclic voltammetry in a presence of 1.0 mM of $Fe(CN)_6^{3-/4-}$ in 0.1M KCl solution in a range of -0.5 to 1.0 V (vs Ag/AgCl) at a scan rate of 100 mV s^{-1} for 2 cycles.

In order to study interfacial property of electrode surface, electrochemical impedance spectroscopy (EIS) was employed on μAUTOLAB type III potentiostat using a solution of 1.0 mM of $Fe(CN)_6^{3-/4-}$ in 0.1M KCl solution with frequency ranging from 0.1 to 10^{-5} Hz and amplitude of 0.01V

3.7 Electrochemical detection

3.7.1 Electrochemical determination of carbofuran and carbendazim

Square-wave voltammetry was employed for simultaneous determination of 20 mg mL^{-1} CBF and 5 mg mL^{-1} CBZ in 0.1 PB solution pH 7.0 under the condition of step potential of 10 mV, amplitude of 20 mV and frequency of 10 Hz, and The peak currents were measured by current integration of each peak obtained from square-wave voltammograms.

3.7.2 Optimization of parameters of square-wave voltammetric measurement

Three important parameters of square-wave voltammetry, namely step potential, amplitude and frequency, were optimized by measuring the SWV responses of 20 mg mL^{-1} CBF and 5 mg mL^{-1} CBZ in 0.1 PB solution pH 7.0 with various conditions. Step potential of 4, 7, 10, 13 and 16 mV, amplitude of 10, 20, 30, 40 and 50 mV and frequency of 5, 10, 15, 20 and 25 Hz were studied. The selected conditions were obtained by that particular condition which provide the high electrochemical responses and well-defined peak shapes.

3.7.3 Analytical performances of modified electrode

3.7.3.1 Calibration plot

Different concentrations ranging of 40-10,000 μg L^{-1} for CBF and 25-5,000 μg L^{-1} for CBZ were prepared in PB solution at pH 7.0. Square-wave voltammetry was performed to determine the mixture solution of CBF and CBZ. Afterwards, calibration

plots were obtained by plotting current response signal versus concentrations of CBF and CBZ.

3.7.3.2 Limit of detection (LOD)

The limit of detection (LOD) was obtained by an evaluation of the level of concentration which provides the signal-to- noise ratio (S/N) of 3:1.

3.8 Real sample analysis

3.8.1 Real sample preparation

Three agricultural products were selected as the real samples including soybean, rice and tomato. They were purchased as raw products from local markets. To prepare the real samples, agricultural product specimens were infused in 50 mL of chloroform and leaved them for a day. Next, 30 mL of chloroform was collected, and removed by a rotary evaporator. Then, 10 mL of ethanol was added instead and collected 5 mL of supernatants to avoid dregs and oil part. Then, CBF and CBZ standard solutions were spiked into the solution. Next, 2 mL of 0.01 M NaOH was mixed together with 5 mL of pesticide solution. The solution was heated up at 85°C in a closed system for 20 minutes, and then cooled down at a room temperature. After that, 2 mL of 0.01 M $HClO_4$ was added to neutralize NaOH. Finally, the pesticide solution was diluted with 41 mL of 0.01 M PB solution pH of 7.0 for a final volume of 50 mL, which has the final concentration of 200, 1,000 and 4,000 µg L^{-1} for CBF and 50, 500 and 2,000 µg L^{-1} for CBZ prior to analyses.

3.8.2 Calculation of percent recovery

For real sample analysis, the percentage of recovery was used for evaluation of method applicability on the purposed system by using external standard method. The percent recovery can be calculated by a following formula:

$$\text{Percent recovery} = \frac{\text{Found concentration of spiked sample}}{\text{Known concentration of spiked sample}} \times 100$$

CHAPTER IV
RESULTS AND DISCUSSION

On this chapter, the results, including electrode surface property and characterization, electrode modification optimization, electrochemical determination and analytical performance of the developed system, were discussed.

4.1 Electrode characterization

4.1.1 Visual characterization

At the beginning, when CTAB was added into GO solution, and the concentration of CTAB is above a critical micelle concentration (CMC), the formation of micellar graphene oxide (MGO) was observed. Thereupon, the process of aggregation of micelles were spontaneously occurred with GO surrounded by CTAB molecules, called micellization. Hydrophilic heads form self-assembly structures, referred as a micelle, to contact aqueous solution, and on the other hand, hydrophobic tail sequesters inward the interior. As shown in Figure 4.1, it exhibits different features of 0.8 mg mL^{-1} of GO solution with varied CTAB concentrations. Firstly, Figure 4.1A shows an appearance of GO solution in the absence of CTAB. An original feature of GO solution was observed as a cloudy and dark-brown solution. Secondly, GO solution appearance in the presence of 0.0025% CTAB remains unchanged as shown in Figure 4.1B, indicating that CTAB micelles are still not formed at this concentration which is below CMC. Thirdly (Figure 4.1C), GO solution was prepared with 0.010% CTAB, and the appearance shows dark-brown micellar sediment of GO suspending in the solution, and micellization takes place by aggregation of CTAB and GO, verifying that the CTAB concentration reaches the CMC. Lastly, the appearance of GO solution at 0.020% CTAB was observed with an increased amount of suspended sediment of GO (Figure 4.1D); thereby, micelles of CTAB-GO are further aggregated with an increasing concentration of CTAB.

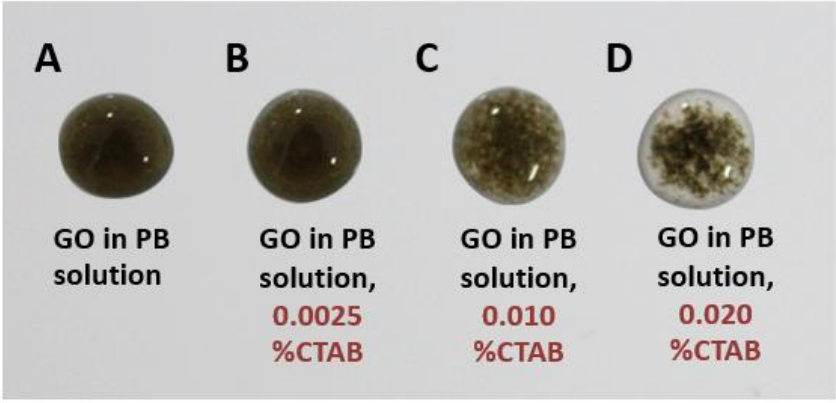

Figure 4.1 Appearances of 50 µL GO solution in an absence (A) and presence of different CTAB concentrations (B-D).

4.1.2 Electrochemical reduction of GO and MGO

To generate ERGO, the electrochemical reducing process was operated by applying highly negative potential to enforce the reduction of oxygen functional groups decorated on the surface of GO sheets. Initially, 0.8 mg mL^{-1} of GO solution was prepared in the absence and presence of 0.010% CTAB. After that, the reducing process was carried out by using cyclic voltammetry scanning in a potential range from -0.5 to -1.7 V (vs Ag/AgCl) with a scan rate of 100 mV s^{-1} for 10 cycles as shown in Figure 4.2. In this work, the cathodic peaks, obtained from cyclic voltammograms, represent 10 cycles of reduction reactions of GO and MGO. The first cycle of cathodic peaks provides the highest current signal, showing that the reduction process of GO takes place almost completely. For the subsequent cycles, the cathodic peaks become lower and vanish because GO exhausts almost entirely. Eventually, reduced GO is cumulatively deposited on the electrode surface. Figure 4.2 shows the comparisons of cyclic voltammograms of reduction reaction between ERGO (blue line) and ERMGO (red line) modified electrode. The cyclic voltammograms of ERGO present that the reduction of GO begins at the potential of -1.0 V and reaches the maximum current at -1.4 V. On the other hand, cyclic voltammograms of ERMGO show that the onset potential of reducing process of MGO is at -0.6 V, and the cathodic peak appears at -1.0 V. Considering the first cycles, ERMGO provides positive shift compared with ERGO, suggesting that a rate of electron transfer is promoted during the process of reducing

MGO. This phenomenon is probably described that the positively charged outer shells of MGO are mainly composed of hydrophilic heads of quaternary ammonium group. Then, the negative potential was applied to the electrode surface, so the positively charged micelles attract the applied negatively charged electrode surface by electrostatic interaction as the resulting of accelerated migration of MGO.

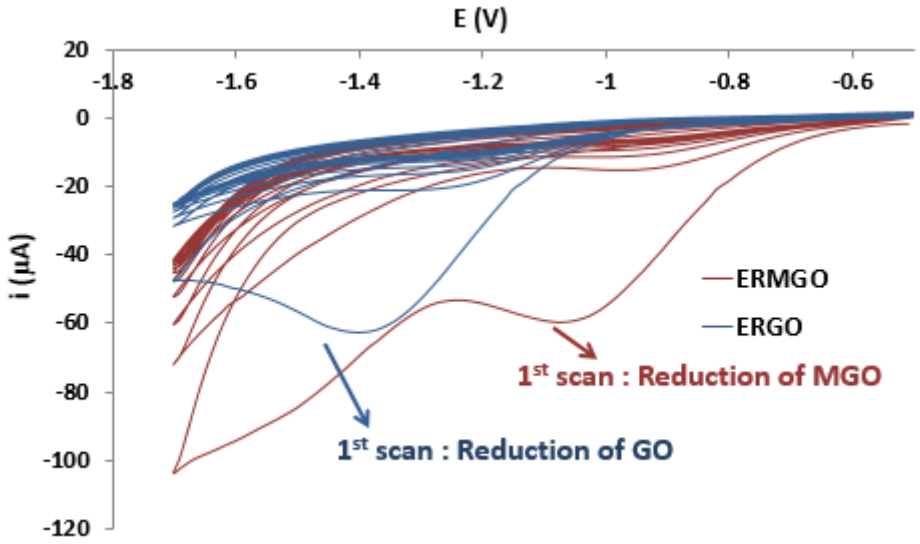

Figure 4.2 Cyclic voltammograms of electrochemical reduction of GO (blue line) and MGO (red line) modified electrode.

In order to prove the successful electrodeposition of RGO on the working electrode surfaces, the surface morphologies of unmodified electrode, ERGO and ERMGO modified electrode were characterized by scanning electron microscopy (SEM) with 1000x magnification as shown in Figure 4.3A-C. According to Figure 4.3A, a SEM image shows a surface morphology of unmodified electrode, exhibiting the sheet-like architecture with plenty of graphite flakes on the electrode surface. Figure 4.3B exhibits a SEM image of ERGO modified electrode that demonstrates ERGO film covering over the sheet-like morphology and concealing all graphite flakes of unmodified electrode. Figure 4.3C displays the morphology of ERMGO modified electrode. Thin ERMGO film also covers over the entire sheet-like morphology. Moreover, ERMGO is a translucent film because it can be seen through the opposite site with vague visibility. Thereby, it

can be concluded that the ERMGO film is more transparent than ERGO film, indicating that ERMGO film is much thinner than ERGO film.

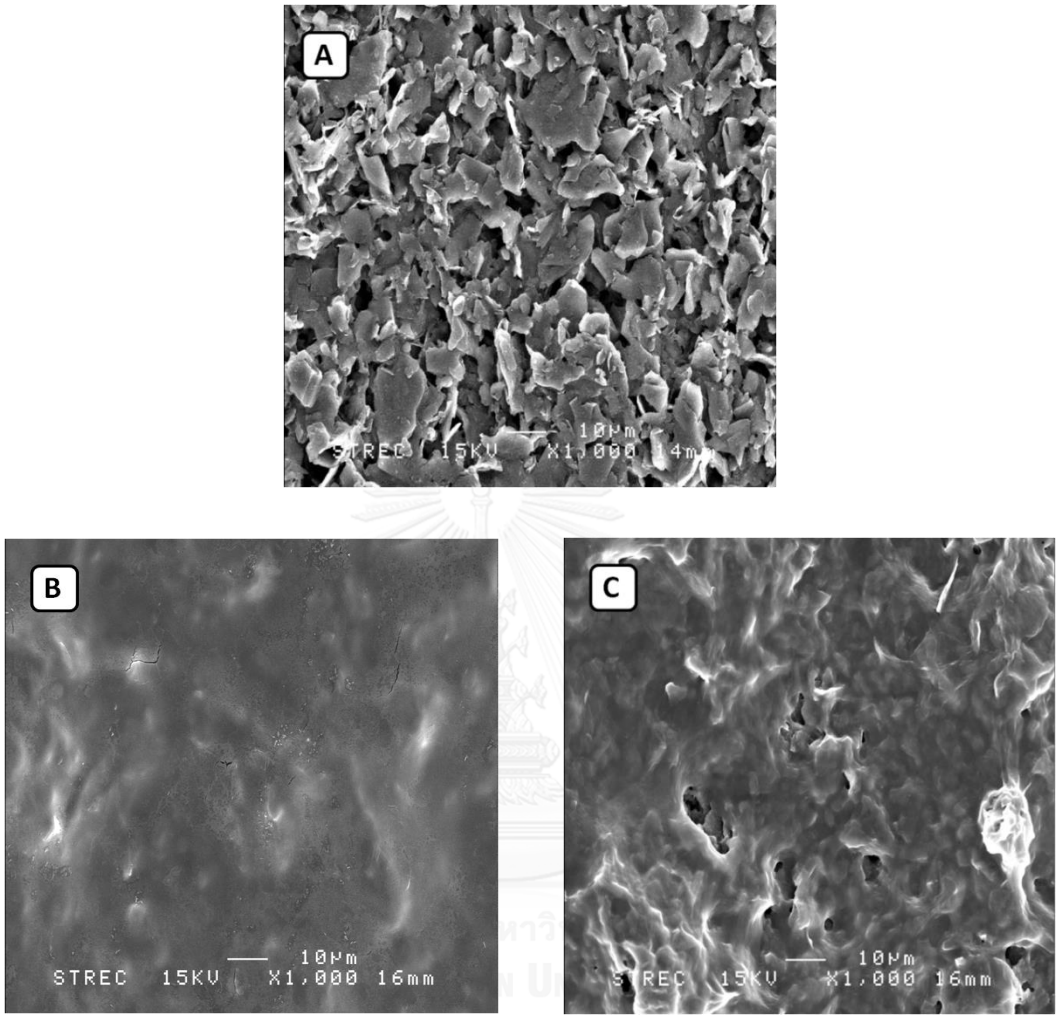

Figure 4.3 SEM images of unmodified working electrode surface (A), ERGO modified working electrode surface (B) and ERMGO modified working electrode surface (C) with a magnification of 1000x.

4.1.3 Contact angle measurement

Contact angle (CA) measurement is one of the techniques used for investigation of the hydrophobic/hydrophilic property or wettability on a solid surface. Contact angle value would be obtained from measuring through the angle formed between the interfaces of dropped water and solid surface. In this work, CA values of an unmodified electrode, ERGO and ERMGO modified electrode surface were measured

using a static sessile drop method as shown in Table 4.1, and the water drop behaviors on the electrode surface were observed as shown in the Figure 4.4A-C. As seen in Figure 4.4A, the water drop behavior on an unmodified electrode surface is almost spherical, and a CA value is found to be 133.18°. Since the CA value obtained from unmodified electrode is larger than 90°, it is considered as a hydrophobic surface. This phenomenon can be described that screened carbon ink composition consists of carbon ink, graphite, graphene flakes, organic solvent and additives *etc*. All the components are hydrophobic, so the unmodified electrode surface repels the water droplet. Likewise, Figure 4.4B displays the water drop behavior on ERGO modified electrode surface. The shape of water drop is also spherical which is similar to the one on an unmodified electrode, and a CA value is found to be 127.52°. Also, ERGO modified electrode surface is classified as hydrophobic surface. As that result, ERGO was generated from the removal of oxygen functionalities on GO sheets by reduction reaction. Consequently, ERGO remains merely entire carbon structure, so it is classified as a hydrophobic surface as well. In contrast, Figure 4.4C shows the water drop behavior on ERMGO modified electrode surface. The water drop pervasively spread over the surface, and a CA value is 68.86°, which is smaller than 90°, indicating that the surface is hydrophilic. This phenomenon can be described that CTAB has a property to reduce the surface tension between interfacial phases. In other words, CTAB has ability of improvement of miscibility between polar and non-polar phases. Thus, the adjustment of ERGO surface with micelle of CTAB takes an advantage of improving compatibility of ERMGO and water.

Table 4.1 Comparison of contact angle values on the surface of different electrodes.

Electrode	Average contact angle values (°± SD)
Unmodified	133.18 ± 2.02
ERGO	127.52 ± 3.51
ERMGO	68.86 ± 3.90

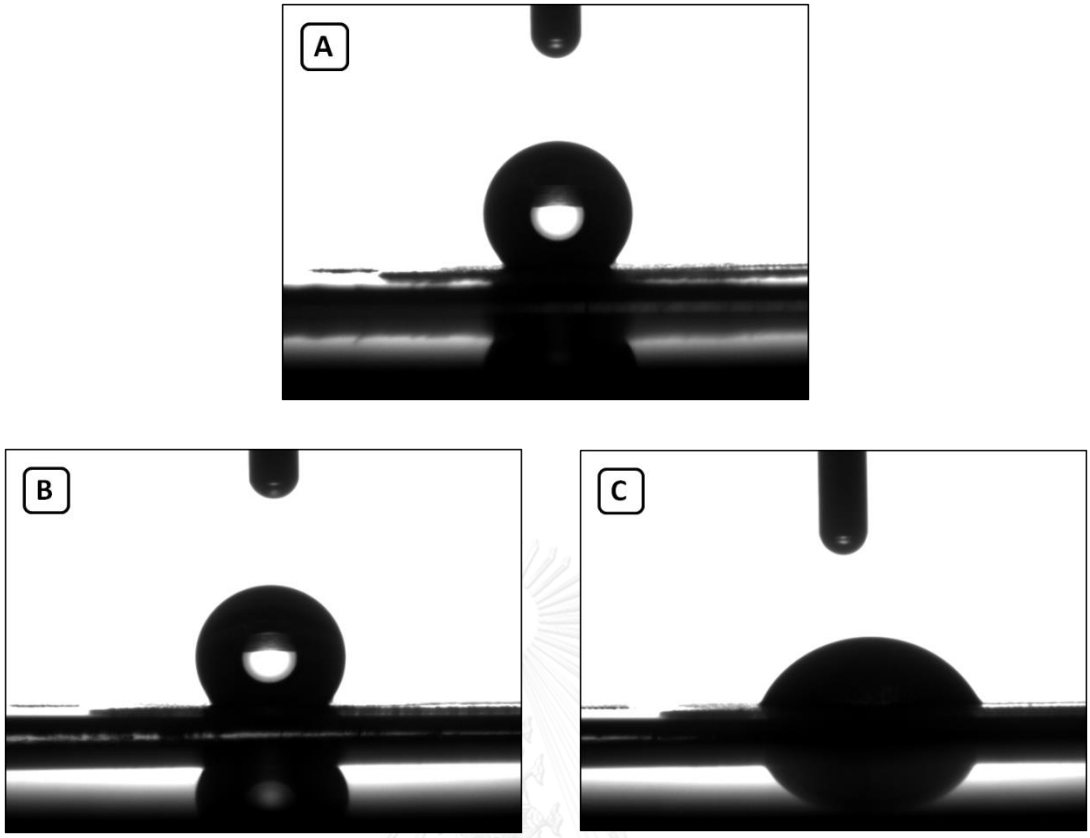

Figure 4.4 Images of water droplet on an unmodified electrode surface (A), an ERGO modified electrode surface (B) and an ERMGO modified electrode surface (C) obtained from CA measurements.

4.1.4 Electrochemical impedance spectroscopy

Also, the interfacial properties of electrode surface were investigated by electrochemical impedance spectroscopy (EIS). The charge-transfer resistance (R_{ct}) depends on dielectric and insulating features at the electrode-electrolyte interface. The R_{ct} value derived from a diameter of semicircle portion of Nyquist plots is related to the charge transfer resistance and electronic resistance of the electrodes. The semicircular portion of Nyquist plots indicates the efficiency of electron transfer from aqueous electrolyte solution to electrode surface. As shown in Figure 4.5, Nyquist plots present the comparison among unmodified electrode (blue line), ERGO modified electrode (green line) and ERMGO modified electrode (red line) in the presence of 1.0 mM of $Fe(CN)_6^{3-/4-}$ in 0.1 M KCl. The Nyquist curve of unmodified electrode shows the largest semicircular portion of all with an R_{ct} value of 16329.4 Ω, indicating that the

unmodified electrode has the highest charge-transfer resistance, leading to poor electron transfer through the surface. For the curve of ERGO modified electrode, the semicircular portion is smaller than unmodified electrode, and an R_{ct} value considerably decreases to 4984.2 Ω. The smaller diameter on the curve indicates that G has an ability to accelerate the electron transfer between electrolyte solution and electrode surface. After modifying the electrode with ERMGO, a semicircular domain does not exist apparently, and the relation is almost straight line; thus, R_{ct} value is not available. This result suggests that the rate of electron transfer on ERMGO modified electrode is very fast. Theoretically, CTAB, surfactant, has no property of direct improvement of the electrical conductivity. For this reason, adding the CTAB might have impeded the electron transfer and obstructed the access of analytes from bulk solution. Thus, the Nyquist curve on ERMGO modified electrode should have possessed the largest semicircular portion. However, ERMGO provides the lowest charge-transfer resistance, implying that CTAB orientation on ERMGO surface facilitates the electron transfer process between ERMGO surface and electrolyte solution.

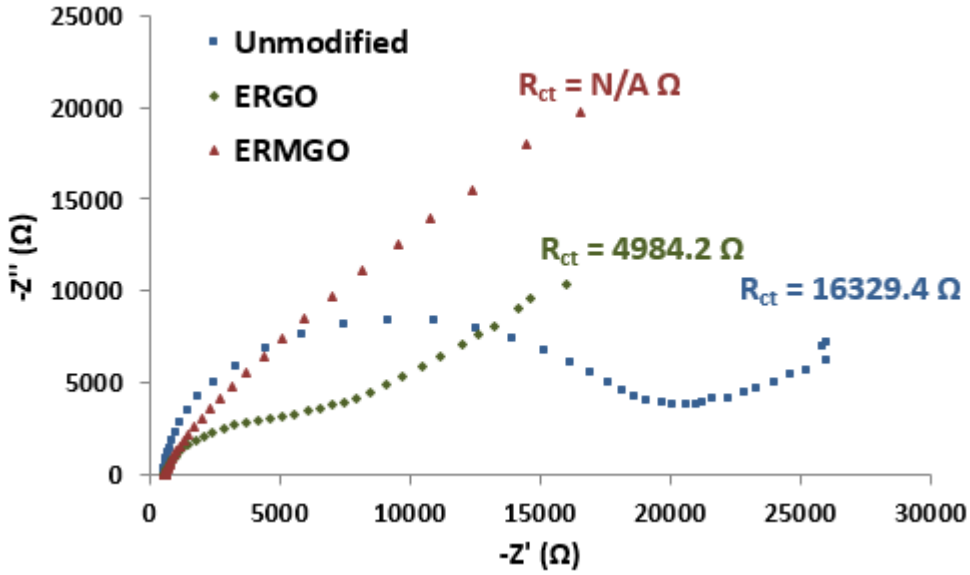

Figure 4.5 EIS of an unmodified electrode (blue), an ERGO modified electrode (green) and an ERMGO modified electrode (red) in the presence of 1.0 mM of $Fe(CN)_6^{3-/4-}$ in 0.5 M KCl.

4.1.5 Cyclic voltammetry

Cyclic voltammetry is a technique used for investigating the electrode performances and characteristics. The electrochemical sensitivity of each electrode model was monitored by measuring a standard solution of 1.0 mM $[Fe(CN)_6]^{3-/4-}$ in 0.1 M KCl which is a standard redox couple commonly used for investigation of the electrocatalytic property of electrode prior to use for target analyte determination. According to Figure 4.6A, this figure shows the voltammograms of 1.0 mM $[Fe(CN)_6]^{3-/4-}$ measured on an unmodified electrode, an ERGO modified electrode and an ERMGO modified electrode. Evidently, all the cyclic voltammograms show anodic and cathodic peaks, and the peak current ratio of both direction are approximately 1.0, defined as reversible redox system. In addition, the Figure 4.6B displays a histogram showing anodic peak currents obtained by current integration of peak from voltammograms. Considering the voltammogram measured on unmodified electrode (green line), it provides the lowest current (25.49 μA) responses and broad peak shapes, and the difference of peak potential value (ΔE_p) is evaluated to be 0.37 V. For the voltammogram measured on ERGO modified electrode (blue line), both anodic and cathodic peak responses are higher and sharper than measured on unmodified electrode. The peak current and the peak potential difference were found to be 43.02 μA and 0.21 V, respectively. This phenomenon can be explained that ERGO on the electrode surface possesses excellent properties; therefore, with higher current responses, it indicates that ERGO electrode surface has more surface area owing to G property. Moreover, the peak potential difference is narrower, suggesting that G on the electrode surface has an ability to promote the electrocatalytic activity. Ultimately, voltammogram measured on ERMGO modified electrode (red line) exhibits the highest and sharpest current response (54.27 μA). Furthermore, it also provides the smallest gap of peak potential (ΔE_p=0.18 V). It is presupposed that CTAB orientation on G surface plays an important part for an increase of electrode surface area and an acceleration of electron transfer process.

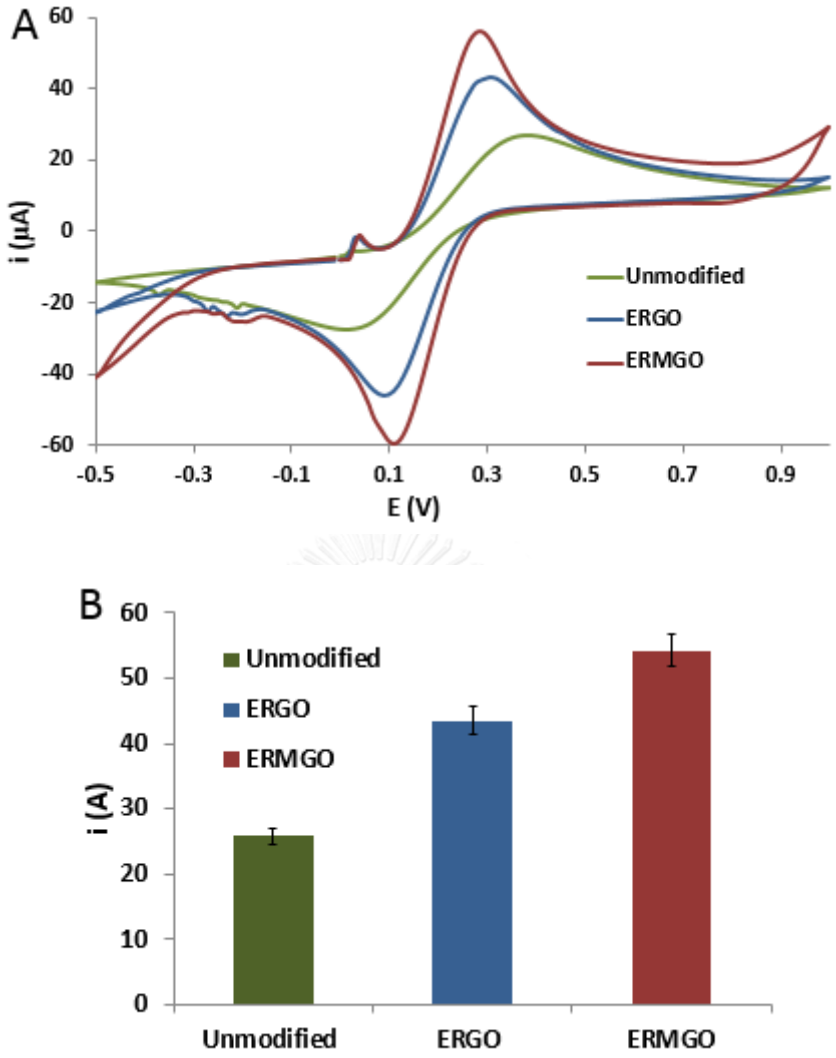

Figure 4.6 Cyclic voltammograms of 1.0 mM $[Fe(CN)_6]^{3-/4-}$ in 0.1 M KCl solution measured on an unmodified electrode (green line), an ERGO modified electrode (blue line) and an ERMGO modified electrode (red line) (A) and a histogram showing anodic peak currents measuring on different electrodes (B).

According to Randles-Sevcik equation, the linear relation between applied square root of scan rates and peak currents can point out that the electrode system is under diffusion-controlled process. To investigate the mass-transfer process of ERMGO modified electrode, the experiments of cyclic voltammetry with different scan rates of 50, 75, 100, 125, 150, 175 and 200 mV s^{-1} were performed to investigate our proposed electrode system as shown in Figure 4.7A. For Figure 4.7B, the anodic and

cathodic peak currents are directly proportional to square root of scan rate. Thus, this electrode platform is in favor of diffusion controlled mass-transfer-process.

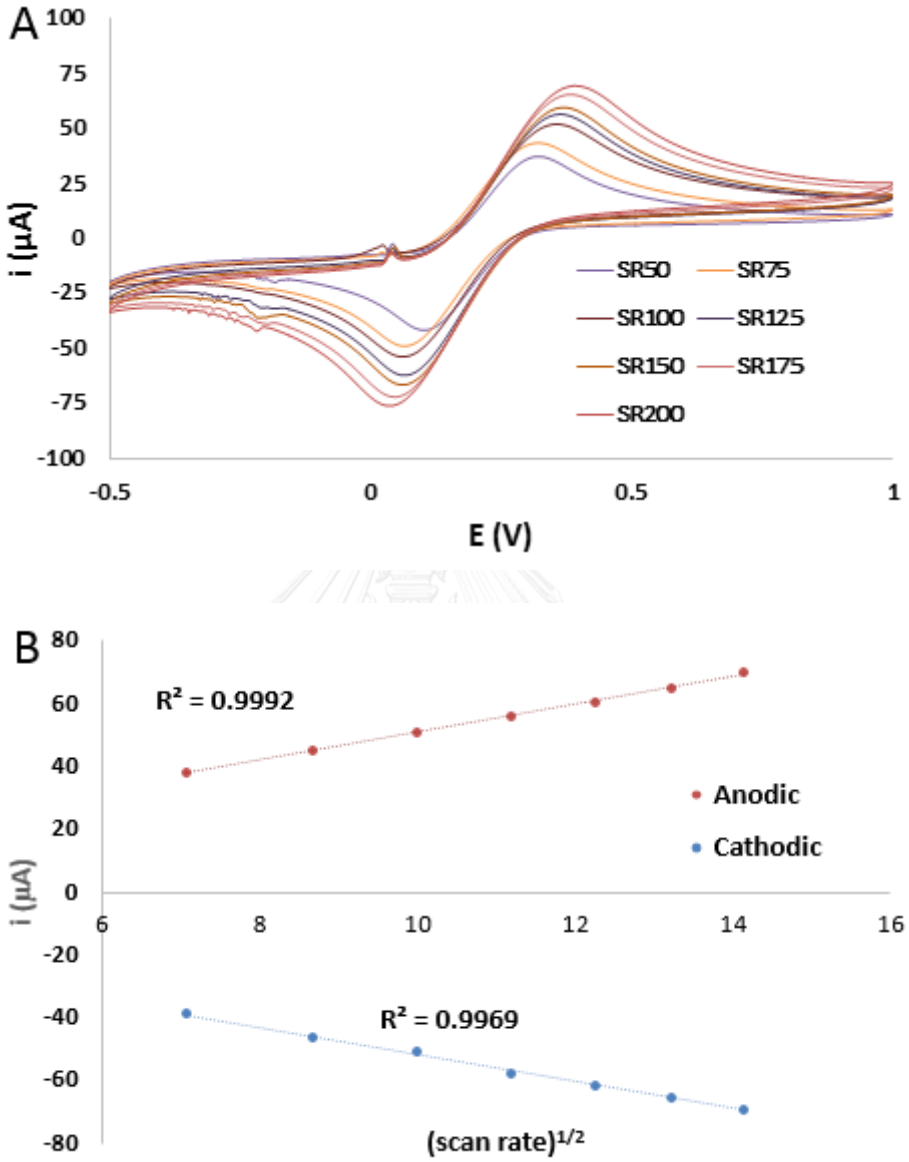

Figure 4.7 Cyclic voltammograms of 1.0 mM $[Fe(CN)_6]^{3-/4-}$ in 0.1 M KCl solution measured on ERMGO modified electrode at the different scan rates of 50, 75, 100, 125, 150, 175 and 200 mV s^{-1} (A) and a relation between anodic and cathodic peak current of $[Fe(CN)_6]^{3-/4-}$ versus a function of square root of scan rate ($\mathbf{V}^{1/2}$) (B)

According to the characterization, although G possesses several exceptional properties, it is still not suitable for directly modifying on electrode surface which is

used to detect analytes in aqueous solution due to water repulsion of hydrophobic G. To bring out the maximum efficiency of G, ERMGO modified electrode was developed. The G surface property was altered by the orientation of micellar CTAB which improves the hydrophilicity of the surfaces. Then, ERMGO modified electrode can improve the compatibility between the analytes and G on the electrode surface, leading to enhanced electron transfer process as a result of high electrode performance.

4.2 Electrochemical determination of CBF and CBZ

In this work, voltammetry is an electrochemical technique which is used for CBF and CBZ detection. However, chemical compounds which are detected by voltammetry must be electroactive species. Unfortunately, only CBZ is an electroactive species (equation 4.1), while CBF has no electrochemical activity (equation 4.2). Therefore, there is a difficulty for direct detection of CBF by using electrochemical method. In previous literature [61], it was reported that carbamate pesticides can produce electroactive phenol derivatives through a process of alkaline hydrolysis at high temperature. As it is, CBF can be hydrolyzed to be CBF phenol (equation 4.3) in the alkalescent aqueous solution. Alternatively, CBF can be determined indirectly by electrochemical detection with CBF phenol (equation 4.4). According to the previous study [62], the factors influencing on the alkaline hydrolysis of CBF was investigated and reported that the optimal conditions for CBF hydrolysis is a hydrolytic temperature of 75^{o}C and a heating time of 3 minutes. In this study, the sample preparation is required and proceeded by heating of the sample solution prior to analyses. Nevertheless, for CBZ properties, CBZ is a high thermal stability compound [65], so it can maintain the original form at high temperature, whereas CBF is hydrolyzed. Ultimately, a prepared mixture solution composed of CBZ and CBF phenol was used for analyses.

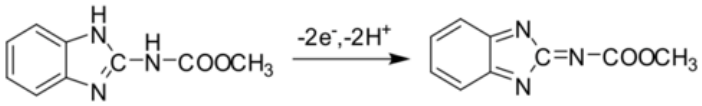

Equation 4.1 Oxidation reaction of CBZ

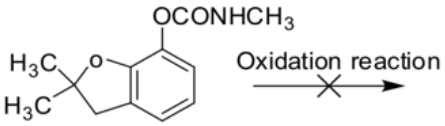

Equation 4.2 Non-electroactive CBF

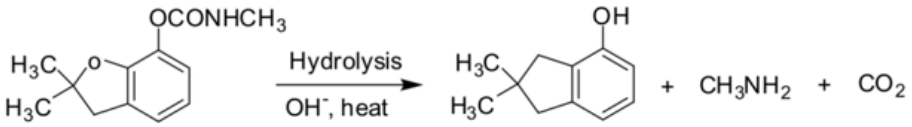

Equation 4.3 Hydrolysis of CBF

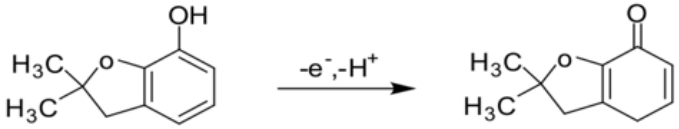

Equation 4.4 Oxidation reaction of CBF phenol

As for the electrochemical detection, square-wave voltammetry (SWV) is selected for the simultaneous determination of CBF and CBZ. Figure 4.8A shows the square-wave voltammograms of 20 mg L^{-1} of CBF and 5 mg L^{-1} of CBZ measured on unmodified electrode (red line), ERGO modified electrode (green line) and ERMGO modified electrode (blue line). The SWV was performed under the condition with a step potential of 10 mV, an amplitude of 20 mV and a frequency of 10 Hz. From the voltammograms, the results present well-separated anodic peaks of two compounds at the potential of 0.18 and 0.53 V belonging to CBF and CBZ, respectively. The peak currents were measured by integration of anodic current responses from each peak as shown in Figure 4.8B. For the voltammogram measured on an unmodified electrode, it shows two anodic peaks which are the lowest current response signal and broadening peak shape. For the current response measured on ERGO modified electrode, the peak currents of both CBF and CBZ are higher than measuring on unmodified electrode, approximately 1.5-fold for CBF and 4-fold for CBZ. The significant increase of current signal can be explained by the excellent properties of G, such as high electrical conductivity, high surface area and well electrocatalytic activity. Then, ERMGO

modified electrodes were used for simultaneous determination of CBF and CBZ. The obtained voltammogram presents the well-defined peaks and have the highest current responses compared to unmodified electrode and ERGO modified electrode. The peak current measured on ERMGO modified electrode is 4-fold higher than unmodified electrode for CBF and 12-fold higher for CBZ. Due to drastic enhancement of current signal, it verifies that ERMGO modified electrode has excellent efficiency for the simultaneous determination of CBF and CBZ.

Besides, the voltammograms implicitly show the background current which is observed by raised curve in a potential range of 0.6 and 1.0 V. The background current obtained from ERMGO modified electrode provide the highest raised curve and followed by ERGO modified electrode and unmodified electrode, respectively. The height of background currents can indicate the double-layer response and capacitance ability. With the higher background current, it shows that the electrode surface has higher capacity.

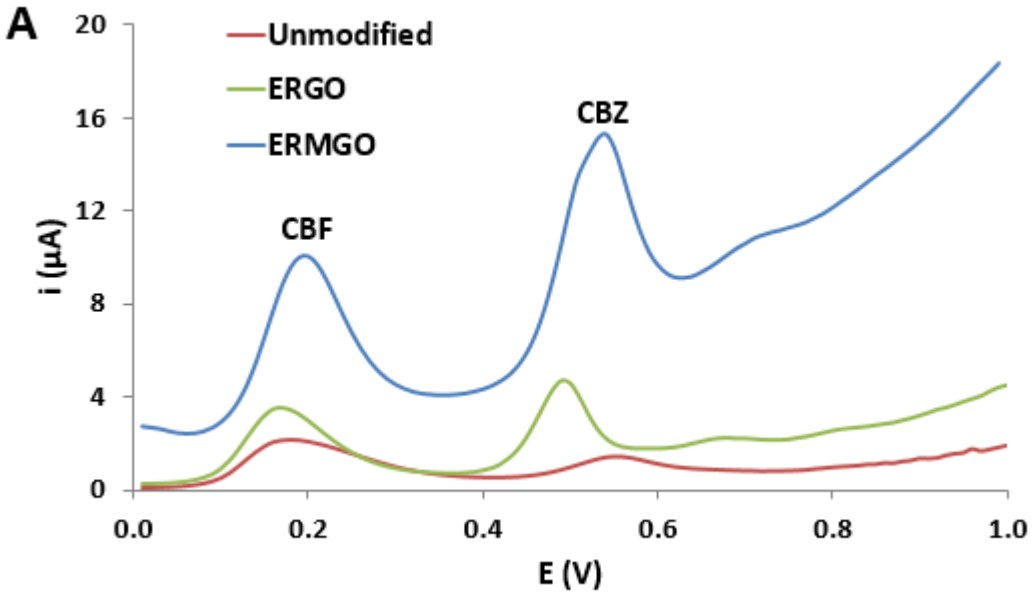

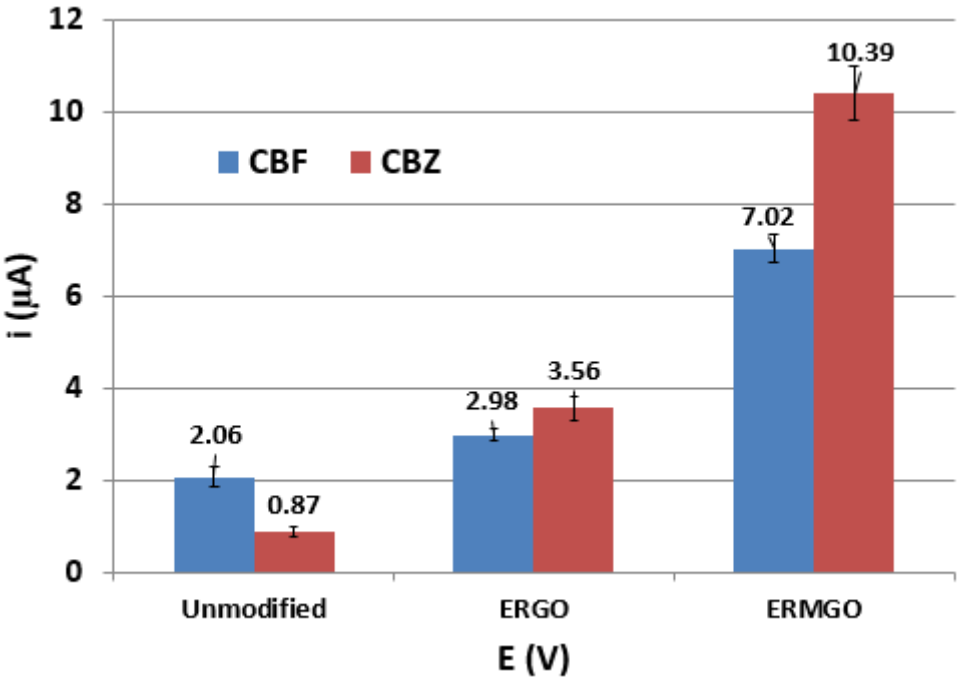

Figure 4.8 Square-wave voltammograms (SWV) of 20 mg L^{-1} CBF and 5 mg L^{-1} CBZ measured on unmodified electrode (blue), ERGO modified electrode (green) and ERMGO modified electrode (red) (A) and a histogram showing peak currents obtained from SWV using unmodified electrode, ERGO modified electrode and ERMGO modified electrode (B).

According to the characterization evidences, the important roles of CTAB orientation on graphene surface, influencing on the electrochemical behaviors, could be explained as follows:

- Due to the hydrogen bonding among oxygen functional groups on GO sheets, GO tends to re-agglomeration. The addition of CTAB can restrain the re-stacking of G because CTAB molecules have a property of reducing surface tension of water and intercalating between dispersed GO sheets, so it has ability to improve GO solubility and dispersibility. Thus, the obtained reduced GO layers dispersed with CTAB are significantly thinner than reduced GO as the result of better electrical conductivity (Figure 4.9).

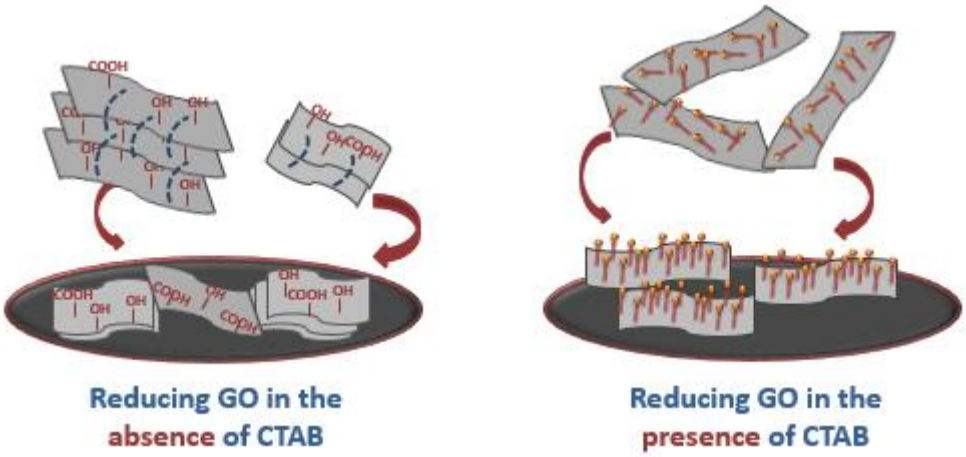

Figure 4.9 CTAB intercalated between graphene oxide sheets can inhibit aggregation during reduction.

- During the electrodeposition of ERMGO on the electrode surface, CTAB on the G sheet will form by orientating the hydrophobic tails towards G and protrude the hydrophilic outwards to the aqueous solution, resulting in decreasing of surface tension of water. In some previous works [66-68], they were reported that the surface tension is related to diffusion coefficient by inverse variation. Consequently, with the decreasing surface tension, diffusion coefficient will contrastingly increase. According to the Randles-Sevcik equation (equation below), the equation shows the relation of current (i_p) and diffusion coefficient (D). The current is directly proportional to the diffusion coefficient.

$$\mathrm{i_p} = (2.69 \times 10^5)\mathrm{n}^{\frac{3}{2}}\mathrm{AD_o}^{\frac{1}{2}}\mathrm{C_o}\upsilon^{\frac{1}{2}}$$

Where n = number of electron transfer, A = electrode surface area (cm^2), C = concentration of the electroactive species (mol cm^{-3}), D = diffusion coefficient (cm^2 s^{-1}) and **V** = scan rate (v s^{-1}).

From the following equation, it is inferred that decreasing surface tension causes of the increase of current. Thus, using ERMGO for CBF and CBZ detection can amplify the current signal, leading to an enhanced sensitivity (Figure 4.10).

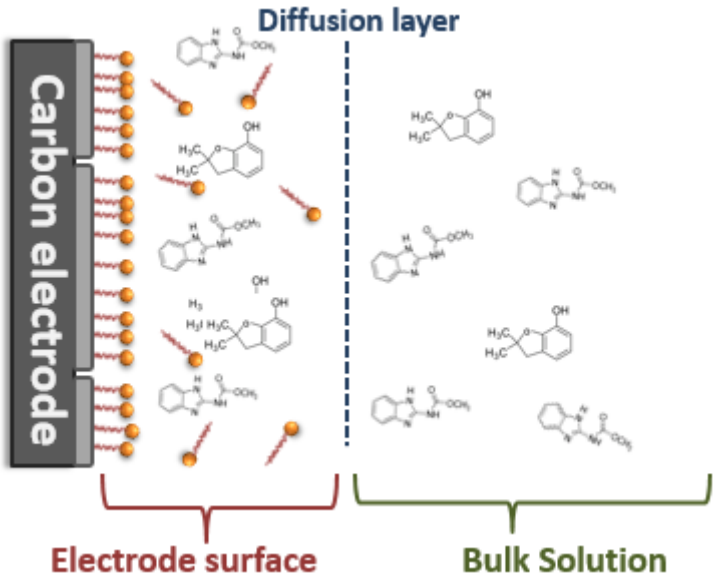

Figure 4.10 CTAB might significantly change the diffusion coefficients.

- From EIS characterization along with CA measurement, because of entire carbon atom of G, the property of ERGO is classified to be hydrophobic. Therefore, using ERGO modified electrode with aqueous solution will create the water resistance between ERGO sheets and water which impedes the electron transfer across the phases. On the contrary, on ERMGO modified electrode, CTAB orientation will diminish hydrophobic effect of G to be hydrophilic surface. Accordingly, the contact of water on ERMGO surface is even more compatible, so the analytes can easily access to the electrode surface. Thereby, it helps to facilitate the electron transfer from ERMGO surface to the electrolyte solution (Figure 4.11).

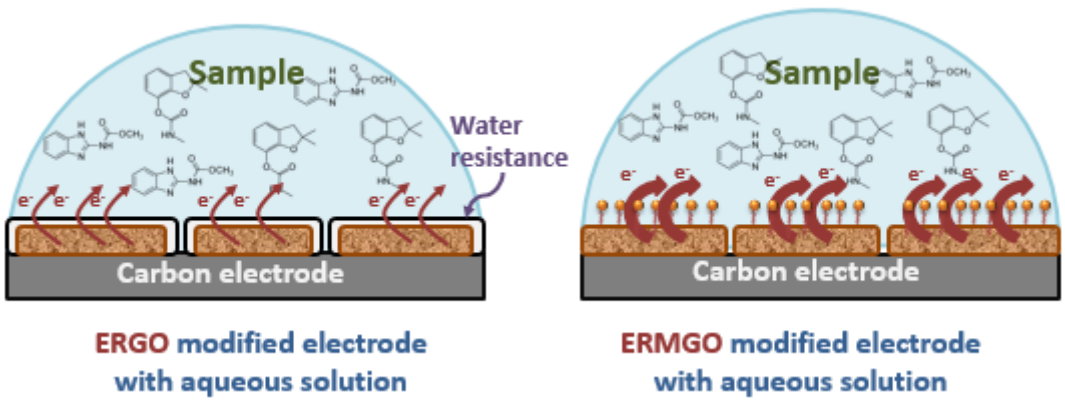

Figure 4.11 CTAB micelle orientation might increase hydrophilicity to the surface of graphene, leading high efficiency of electron transfer.

According to Randles-Sevcik equation (equation 4.5), it is obvious that the electrode surface area is directly proportional to the peak current. For increasing of sensitivity, many developers enhanced electrochemical sensitivity by increasing surface area of electrode, for example, using high surface area materials (*i.e.* nanoparticles [11, 12, 69]) or modifying working electrode surface (*i.e.* electrospraying [70, 71] or electrospinning [72, 73]). Nonetheless, diffusion coefficient is also one of the factors providing a direct effect on current response signal, but the diffusion coefficient is supposed to be a characteristic of each compound. Thus, they are oblivious of improving of diffusion coefficient. However, ERMGO modified electrode platform is the system which improves both surface area and diffusion coefficient.

4.3 Optimization of ERMGO modified electrode fabrication

4.3.1 Effect of GO concentration

To fabricate ERMGO modified electrode, the important parameters concerning in MGO solution, including CTAB concentration, GO concentration, scan rate and number of scan of cyclic voltammetry during reducing process, were optimized. The selected conditions were obtained from that particular condition which provides both highest peak current and well-defined peak shape. First of all, GO concentration in MGO solution was optimized. The GO concentration was investigate within concentrations of 0.5, 0.6, 0.7, 0.8, 0.9 and 1.0 mg mL^{-1} as shown in Figure 4.12A. The current responses continuously increase until the concentration reaches to 0.8 mg mL^{-1}, and then it plateaus; thus, 0.8 mg mL^{-1} of GO was selected as an optimum concentration.

4.3.2 Effect of CTAB concentration

CTAB concentration in MGO solution was varied within a concentration range of 0.0025, 0.005, 0.010, 0.015 and 0.020 %w/v compared with the absence of CTAB as shown in Figure 4.12B. As the result, at the condition without CTAB, peak currents of CBF and CBZ show the lowest signal. After adding CTAB, the current responses of both

analytes significantly increase. At the concentration of 0.0025 % CTAB, the current of CBF slightly increase as the current of CBZ dramatically increases. After varying the concentration of CTAB from 0.005 to 0.020 %, the current responses of CBF rapidly increase, while the current responses of CBZ slightly decrease. Obviously, CBF response to CTAB is higher than CBZ response. The level off and drop of peak current with increasing CTAB concentration can be explained by the predomination of raised background leads to the lower peak current integration than it should have been (Figure 4.13). According to these results, the compromising selection of this parameter is 0.010 % for preparation of MGO solution.

4.3.3 Effect of scan rate

Afterwards, in the process of reducing MGO, the parameter of scan rate was optimized as shown in Figure 4.12C. The different scan rates of 50, 100, 150 and 200 mV s^{-1} were used for studying the effect of scan rate on electrochemical sensitivity. At the slowest scan rate of 50 mV s^{-1}, it provides the highest current responses of CBF and CBZ. Then, with increasing scan rate to be 100, 150 and 200 mV s^{-1}, the current signals slightly decrease. Therefore, at the scan rate of 100 mV s^{-1} was selected for an optimal scan rate by consideration of time consumption of reducing process and adequately high current signal.

4.3.4 Effect of number of scans

Lastly, the effect of different number of scan was investigated by an operation of cyclic voltammetry with the number of scan of 5, 6, 7, 8, 9 and 10 cycles. As shown in Figure 4.12D, the peak currents slightly increase when the number of scan increases. With greater number of scan of cyclic voltammetry, an accrual of G deposition is more accumulative, resulting in increase of anodic peak currents. The selected condition would be considered from the condition which is obtained from the suitability of compromise between the current response and operation time. Then, the optimal conditions of 10 cycles were chosen for further experiments.

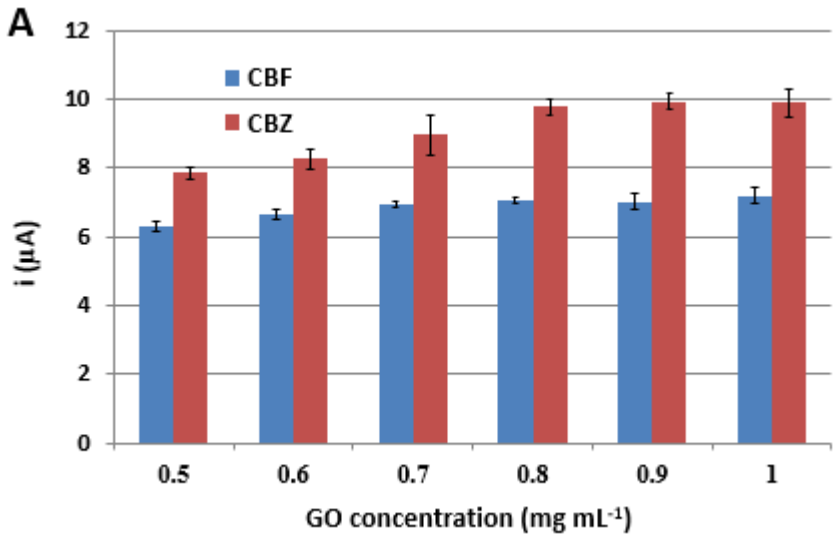
A
CBF
CBZ
i (µA)
0
2
4
6
8
10
12
0.5
0.6
0.7
0.8
0.9
1
GO concentration (mg mL-1)

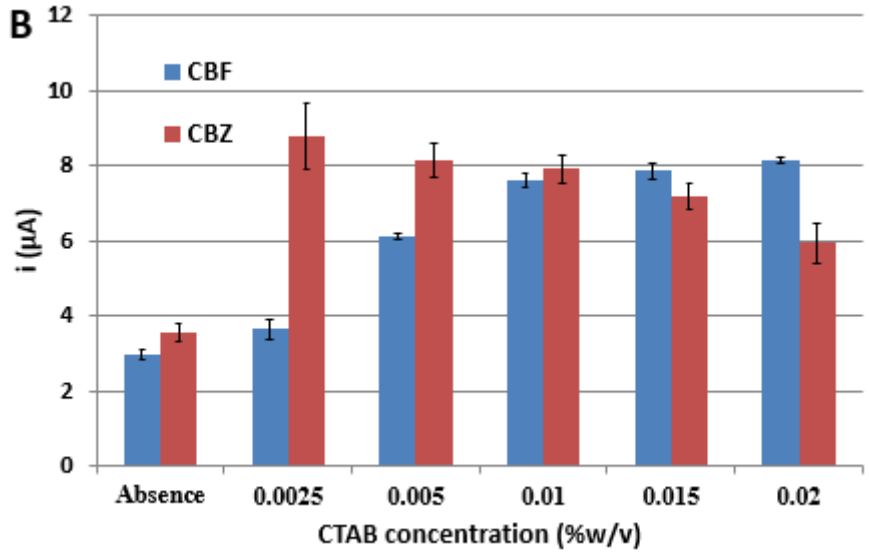
B
CBF
CBZ
i (µA)
0
2
4
6
8
10
12
Absence
0.0025
0.005
0.01
0.015
0.02
CTAB concentration (%w/v)

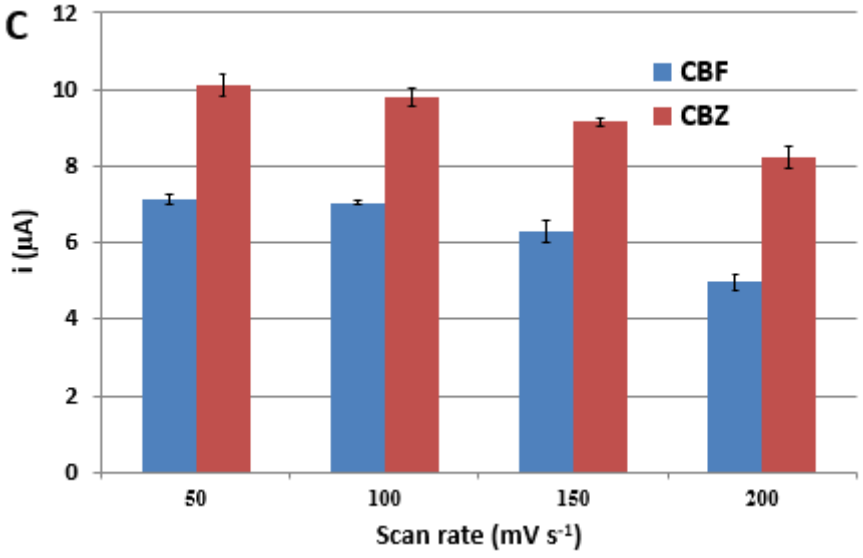
C
CBF
CBZ
i (µA)
0
2
4
6
8
10
12
50
100
150
200
Scan rate (mV s-1)

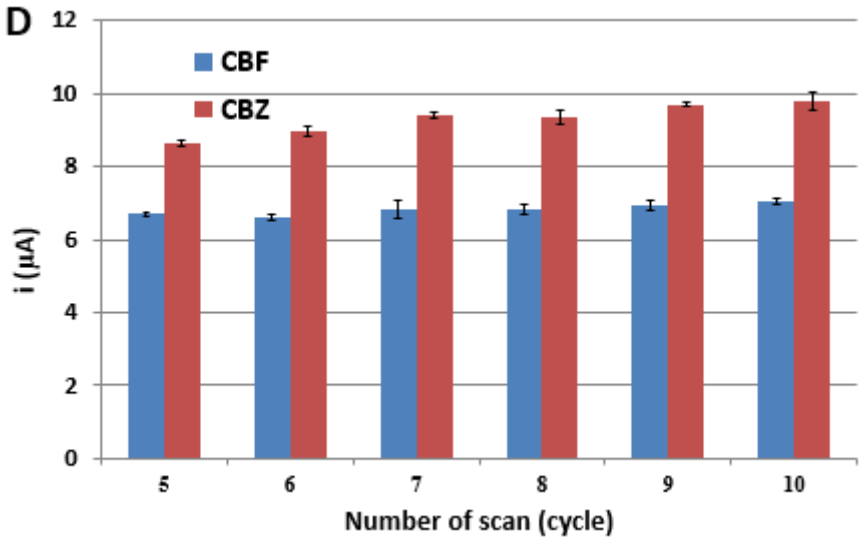

Figure 4.12 Optimization of GO concentration (mg mL^{-1}) using ERMGO modified electrode (A) of CTAB concentration (%w/v) using ERMGO modified electrode (B) of scan rate (mV s^{-1}) (C) of number of scan (cycle) (D).

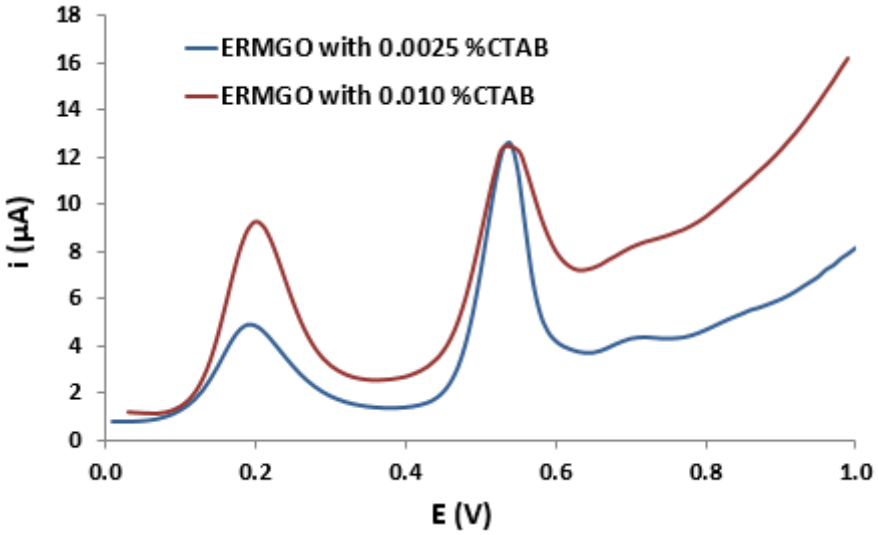

Figure 4.13 SWV of CBF and CBZ measured on ERMGO modified electrode with 0.0025% CTAB (blue line) and 0.010% CTAB (red line).

Three important parameters of SWV, step potential, amplitude and frequency, were optimized in order to observe the proper condition which contributes to the most excellent sensitivity of simultaneous determination of CBF and CBZ. The selection of optimal conditions were based on the particular condition providing the

compromise among well-separated and sharp peaks and high current signals with low background current. For the optimization of these parameters, including step potential of 4-16 mV, amplitude of 10-50 mV and frequency of 5-25 Hz were varied with 20 mg mL^{-1} CBF and 5 mg mL^{-1} CBZ in 0.1 M PB solution (pH 7.0). As shown in the Figure 4.14A, the operation of SWV with 10 mV provides high and well-separated peak shapes, so 10 mV of step potential was selected. For the optimization of amplitude (Figure 4.14B), the current responses at 20 mV provides the suitably high peak current and narrow peak with low background current. Therefore, 20 mV of amplitude was chosen. Finally, for the optimization of frequency (Figure 4.14C), the current responses at 10 Hz of frequency are the sharpest, and the background current is the lowest, so 10 Hz of frequency was selected. Thereby, the optimal condition of SWV for CBF and CBZ determination was the step potential of 10 mV, the amplitude of 20 mV and the frequency of 10 mV and this condition will be used for further experiments.

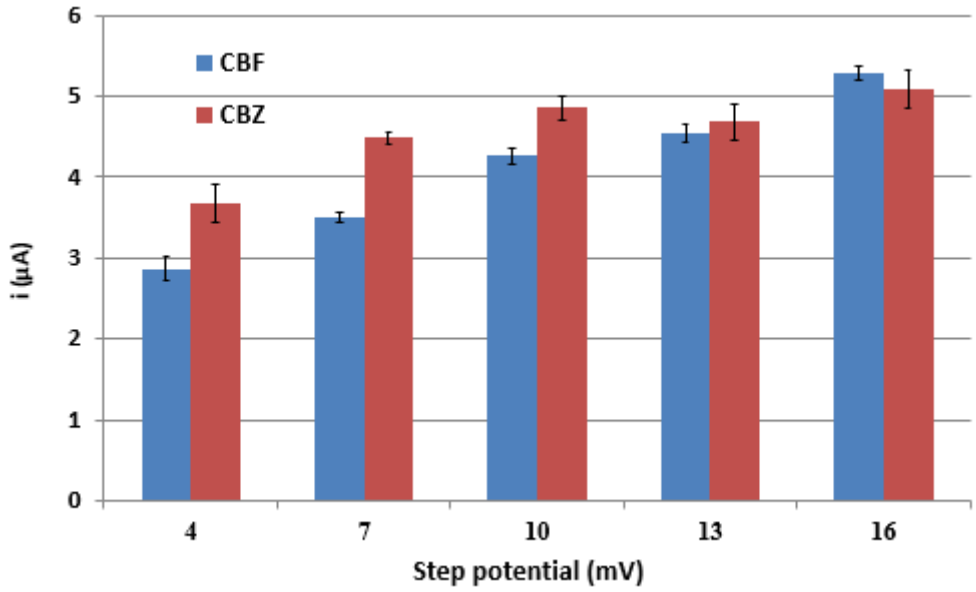

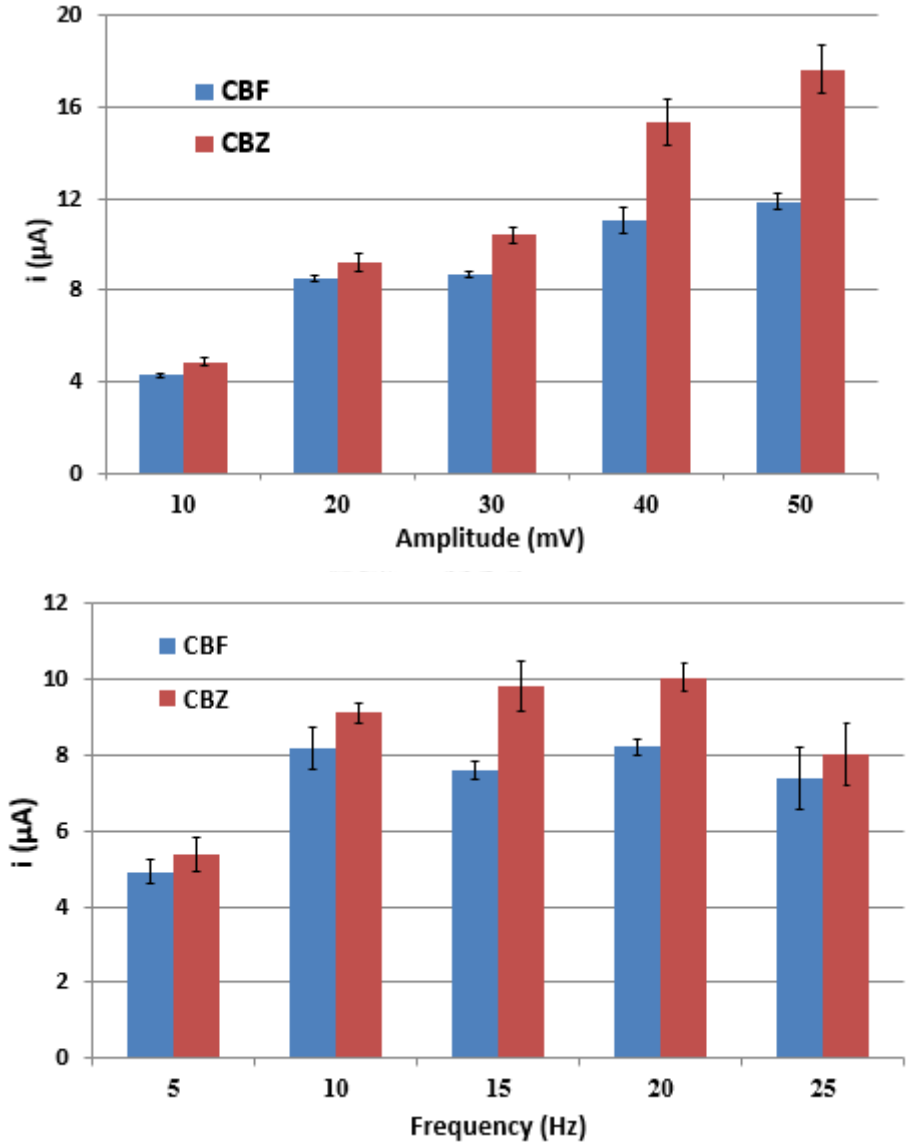

Figure 4.14 Histograms showing anodic current responses obtained from optimizations of SWV parameters: step potential (A) amplitude (B) and frequency (C) measured on ERMGO modified electrode with 20 mg mL^{-1} CBF and 5 mg mL^{-1} CBZ in 0.1M PB solution (pH 7.0).

4.4 Analytical performances of ERMGO modified electrode

The analytical performances of ERMGO modified electrode for the simultaneous determination of CBF and CBZ were evaluated. To investigate the detection capability, different concentrations of analytes were determined for five replicates (n=5) at a concentration range of 40, 100, 200, 400, 1000, 2000, 4,000, 10,000

and 20,000 µg L^{-1} for CBF and 25, 50, 100, 250, 500, 1,000, 2,500 and 5,000 µg L^{-1} for CBZ (Figure 4.15A). The calibration curves of CBF and CBZ were plotted, and the current responses increase linearly with the increase of analyte concentrations. As for CBF detection, a calibration plot (Figure 4.15B) is linear over a range of 40-20,000 µg L^{-1} with a correlation coefficient (R^2) of 0.997. On the other hand, a calibration curve of CBZ (Figure 4.15C) was obtained over a range of 25-5,000 µg L^{-1} with a correlation coefficient (R^2) of 0.994. The experimental limit of detection (LOD) was evaluated based on signal-to-noise ratio of three (S/N=3), and LODs were found to be 10 and 5 µg L^{-1} for CBF and CBZ, respectively. According to maximum acceptable amounts of CBF and CBZ from Maximum Residue Limits (MRLs), there are 50-2,000 µg L^{-1} for CBF and 50-15,000 µg L^{-1} for CBZ. Apparently, LODs obtained from ERMGO modified electrode are below the regulation; thus, this system is sufficiently sensitive for the simultaneous determination of CBF and CBZ in real agricultural products.

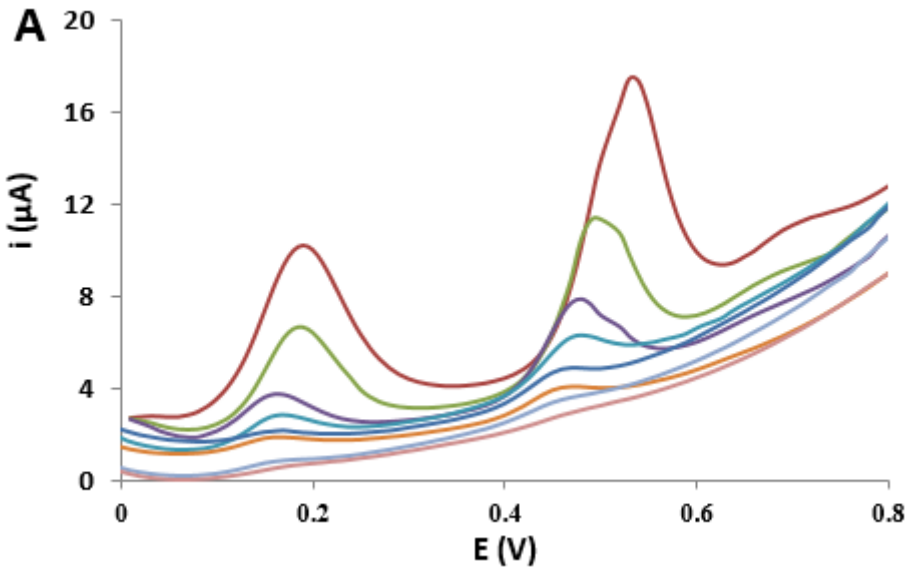

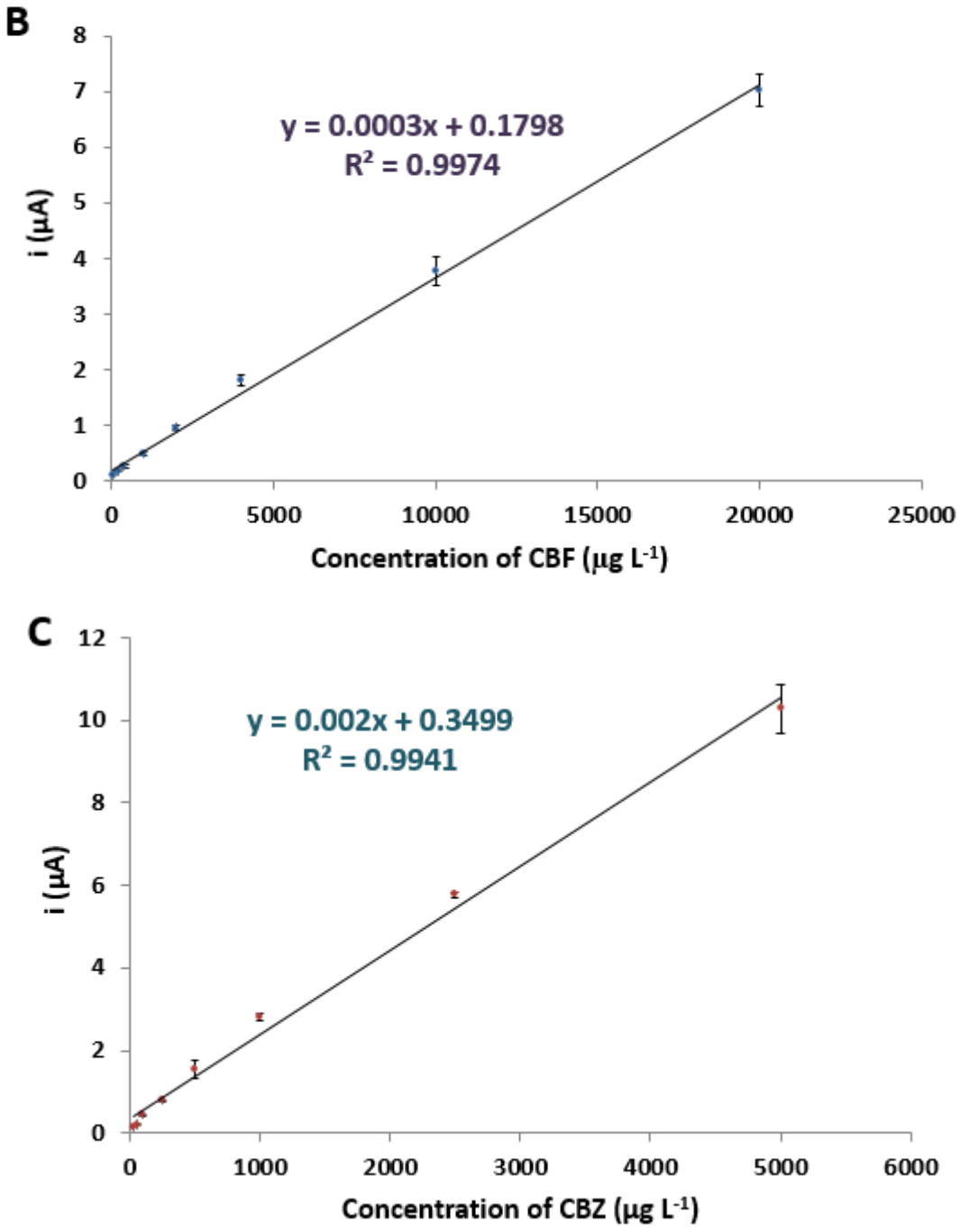

Figure 4.15 Square-wave voltammograms of CBF and CBZ in a concentration range of 40-10,000 µg L^{-1} and 25-5,000 µg L^{-1} , respectively, in PB solution at a pH 7.0 (A), a calibration plot of CBF concentrations versus current signal (B) and a calibration plot of CBZ concentrations versus current signal (C).

The comparison of the analytical performances of this proposed system with the previously reported system are shown in Table 4.2 and 4.3. Comparing with the previous works, our system provides the competent analytical performances for simultaneous determination of CBF and CBZ. Interestingly, by comparing with the similar platforms, our system provides lower LOD and wider linear range. Moreover, the most important purpose of modifying screen-printed carbon electrode is using for disposable sensors. Therefore, it will be somewhat futile if the electrodes were modified with noble metal nanoparticles (gold nanoparticles, cobalt phthalocyanine *etc.*) or high-cost materials (diamond electrode *etc.*) or complicated preparation (molecular imprinting *etc.*) or double/triple modification steps. As seen, the materials used for electrode modification in our system are much simpler and cheaper than others. In addition, the preparation procedure is a one-step operation of electrodeposition, so several advantages of our system are appraised to be a simple and rapid preparation.

Table 4.2 Comparison of the purposed electrode with other modified electrodes in the determination of CBF.

Modified electrode	Method	Supporting electrolyte	Linear range (μg L-1)	Detection limit (μg L-1)	Other analytes	References
Co-RGO/ GCE	DPV	0.1M B-R (pH4): acetonitrile	95.5-13,370	3.82	Carbaryl (simultaneous)	[74]
MIP-RGO@ Au/GCE	DPV	0.1 M KCl	9.55-3,820	3.82	-	[75]
Heated –SPCE	DPV	Borate buffer (pH 10)	76.4-76,400	9.55	-	[62]
Micellar CTAB-RGO/SPCE	SWV	PB solution (pH 7.0)	40-20,000	10	Carbendazim (simultaneous)	This work

Table 4.3 Comparison of the purposed electrode with other modified electrodes in the determination of CBZ.

Modified electrode	Method	Supporting electrolyte	Linear range ($\mu g\ L^{-1}$)	Detection limit ($\mu g\ L^{-1}$)	Other analytes	References
SiO_2 MWNTs/GCE	SWV	0.1M PB Solution (pH 8)	38.2-764	11	-	[76]
MWNTs-PMRE/GCE	LSV	0.6M H_2SO_4	38.2-1,910	1.7	-	[77]
GO-MWNTs/GCE	DPV	B-R solution (pH 1.8)	1.91-764	1.0	-	[78]
Diamond electrode	SWV	0.1M Na_2HPO_4 (pH 2)	95.5-2,865	22	-	[79]
TCP/SPCE	Stripping -DPV	B-R solution (pH 4.0)	95.5-1,910	57.3	-	[80]
G/SPCE	Stripping -SWV	1.0M $HClO_4$	500-10,000	110	Isoproturon (simultaneous)	[81]
Micellar CTAB-RGO/SPCE	SWV	PB Solution (pH 7.0)	25-5,000	5	Carbofuran (simultaneous)	This work

4.5 Interference study

Sample preparation is a crucial step to eliminate interferences, especially for real sample analyses. In this study, the crop specimens were initially infused in chloroform for extraction of pesticides. This step was carried out to avoid ions and polar compounds (*e.g. ascorbic acid*) which can potentially interfere the analyte detection. After extraction by chloroform, the infusions were resolvated by ethanol, and then collected a clear part from ethanol solution for elimination of dregs and other non-polar compounds (*e.g. pigment oils*). It can be presumed that prepared samples do not have any interference, proved by ascertaining that the current signal of CBF and CBZ in standard solution and real samples, which had been already prepared, are perfectly matched at every concentration level (Figure 4.16). Thus, a real sample analysis can be determined by using an external standard method.

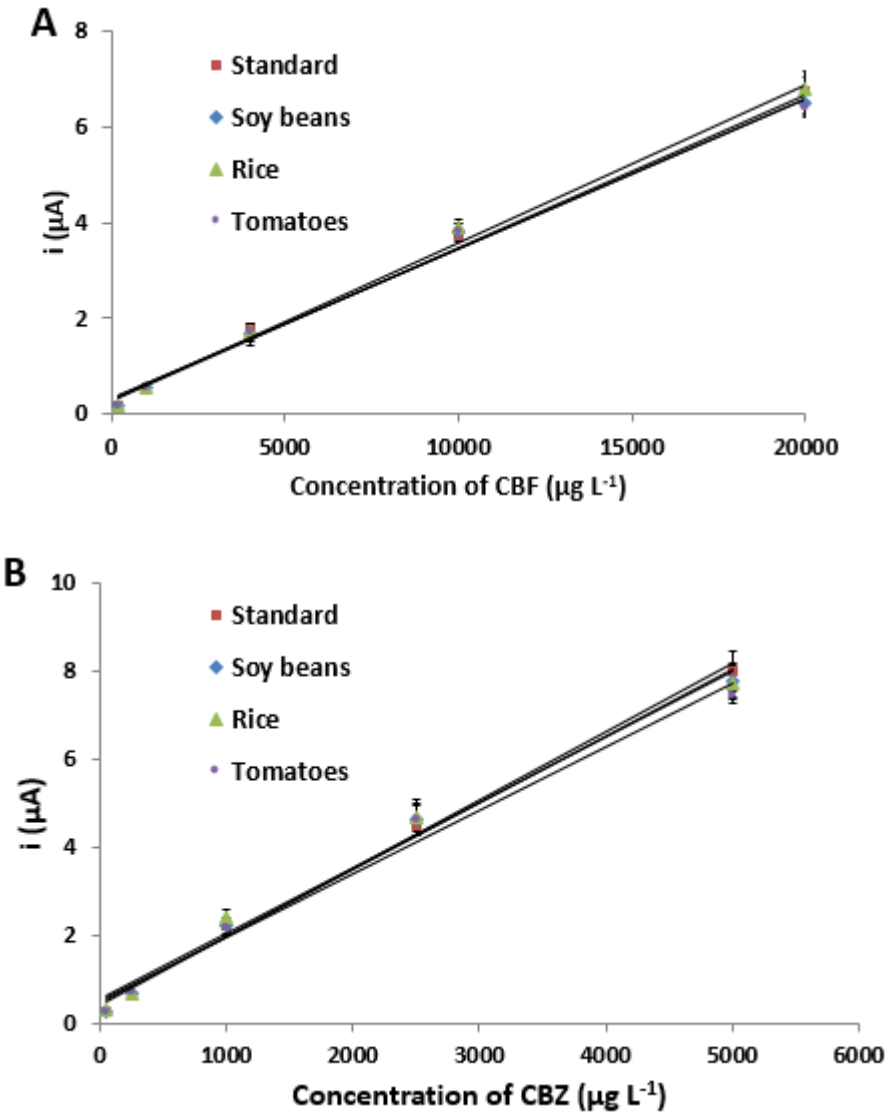

Figure 4.16 Matchings of peak currents among CBF (A) and CBZ (B) in standard solution and real sample solutions (soy beans, rice and tomatoes) at every concentration level measured on ERMGO modified electrode.

4.6 Real sample analyses

To validate applicability of our developed system, ERMGO modified electrodes were applied for the simultaneous detection of CBF and CBZ in real samples. Three types of agricultural products which have possibility of being contaminated by both pesticides were selected as real samples, namely soy beans, rice and tomatoes. For our analytical method, three levels of pesticide concentration were spiked into the

real samples. For CBF, there are concentrations of 200, 1,000 and 4,000 μg L^{-1} added into the real samples. Likewise, 50, 500 and 2,000 μg L^{-1} of CBZ were spiked. Afterwards, the amounts of these pesticides in the real samples were determined by external standard method. Each sample was detected thrice (n=3), and the average values are shown in table 4.4 and 4.5. The percent recoveries were found in the ranges of 95-102% and 97-103% for CBF and CBZ, respectively. The percent RSD is significantly acceptable in every single range of concentration according to a standard AOAC guideline [82], indicating that this developed system can be successfully applied for simultaneous determination of CBF and CBZ in the actual agricultural samples with high accuracy and precision.

Table 4.4 Determination of CBF in three agricultural crop samples using ERMGO modified electrode (n=3).

Samples	Concentration (μg L^{-1})		Recovery (%)	RSD (%)
	Added	Found		
Soy bean	4,000	4,023.50±227.98	100.59	5.66
	1,000	997.67±46.67	99.77	4.68
	200	191.42±7.68	95.71	3.99
Rice	4,000	4,033.20±239.36	100.83	5.93
	1,000	994.33±65.66	99.43	6.60
	200	207.88±12.14	102.79	5.84
Tomato	4,000	3917.70±63.86	97.74	1.63
	1,000	974.33±58.41	97.43	5.99
	200	199.75±15.61	99.87	7.81

Table 4.5 Determination of CBZ in three agricultural crop samples using ERMGO modified electrode (n=3).

Samples	Concentration (μg L^{-1})		Recovery (%)	RSD (%)
	Added	Found		
Soy bean	2,000	2,072.30±41.66	103.61	2.01
	500	527.63±10.95	105.53	2.08
	50	97.00±6.61	97.00	6.82
Rice	2,000	2,065.10±104.18	103.26	5.04

	500	517.42±15.44	103.48	2.98
	50	101.17±4.02	97.78	3.97
Tomato	2,000	2,046.80±74.10	102.33	3.62
	500	502.00±15.44	100.40	0.99
	50	99.08±9.36	99.08	9.45

CHAPTER V
CONCLUSION

5.1 Conclusion

ERMGO modified SPCE was developed as a novel platform of high performance electrochemical sensor for sensitive and simultaneous determination of CBF and CBZ. The use of G along with CTAB improved both electrode surface area and diffusion coefficient, leading to substantially increased electrochemical sensitivity of the system. By using ERMGO modified electrode along with SWV, linear ranges of 40-20,000 μg L^{-1} and 25-5,000 μg L^{-1} were obtained for CBF and CBZ, respectively. The detection limits (LODs) were found to be 10 μg L^{-1} for CBF and 5 μg L^{-1} for CBZ. Ultimately, this system was successfully applied for the determination of pesticide residues in real agricultural crops with high accuracy and precision. Besides, this system can be created with fast and simple fabrication process with low cost. Thus, it might be an interesting prototype for electrode modification using ERMGO with other materials for other application fields.

5.2 Suggestion for future work

This conception of using micelle of nanoparticles can be applied for other applications; for example, it can be used with other carbon-based nanoparticles because others also have the same property of hydrophobicity, or ERMGO can be used along with other material for multiple modification electrode to further increase electrochemical sensitivity.

REFERENCES

[1] Moraes, F.C., Mascaro, L.H., Machado, S.A.S., and Brett, C.M.A. Direct electrochemical determination of carbaryl using a multi-walled carbon nanotube/cobalt phthalocyanine modified electrode. Talanta 2009. **79**: 1406-1411.

[2] Marshall, H. Carbendazim. Pesticides News. Vol. 57, 2002.

[3] Li, Q.X., Hammock, B.D., and Seiber, J.N. Development of an enzyme-linked immunosorbent assay for the herbicide bentazon. Journal of Agricultural and Food Chemistry 1991. **39**: 1537-1544

[4] Toxicity Section, B.V.C., Murray State University, Hopkinsville, Kentucky. Carbofuran toxicity. 1994: Journal of Toxicology and Environmental Health. 383-418.

[5] Moral, A., Sicilia, M.D., Rubio, S., and Pérez-Bendito, D. Multifunctional sorbents for the extraction of pesticide multiresidues from natural waters. Analytica Chimica Acta 2008. **608**: 61-72.

[6] Fu, G.N., He, Y.Z., Yu, C.Z., Gao, Y., and Gan, W.E. Preconcentration and Determination of Carbamate Pesticide Residues in Vegetable Samples by Electrokinetic Flow Analysis with On-Line Hollow Fiber Liquid–Liquid–Liquid Microextraction and Spectrophotometry. Spectroscopy Letters 2009. **42**: 305-311.

[7] Xu, X.m., et al. Distribution and migration study of pesticides between peel and pulp in grape by online gel permeation chromatography–gas chromatography/mass spectrometry. Food Chemistry 2012. **135**: 161-169.

[8] Godejohann, M., Berset, J.D., and Muff, D. Non-targeted analysis of wastewater treatment plant effluents by high performance liquid chromatography–time slice-solid phase extraction-nuclear magnetic resonance/time-of-flight-mass spectrometry. Journal of Chromatography A 2011. **1218**: 9202-9209.

[9] Wen, Y., et al. Salting-out assisted liquid–liquid extraction with the aid of experimental design for determination of benzimidazole fungicides in high

salinity samples by high-performance liquid chromatography. Talanta 2013. **106**: 119-126.

[10] Álvarez, J.D., Vivas, M.M., Gómez, D.G., Gonzalo, E.R., and Martínez, R.C. Capillary electrophoresis coupled to mass spectrometry for the determination of anthelmintic benzimidazoles in eggs using a QuEChERS with preconcentration as sample treatment. Journal of Chromatography A 2013. **1278**: 166-174.

[11] Bernalte, E., Marín Sánchez, C., and Pinilla Gil, E. Gold nanoparticles-modified screen-printed carbon electrodes for anodic stripping voltammetric determination of mercury in ambient water samples. Sensors and Actuators B: Chemical 2012. **161**: 669-674.

[12] Pal, M. and Ganesan, V. Electrochemical determination of nitrite using silver nanoparticles modified electrode. Analyst 2010. **135**: 2711-6.

[13] Goyal, R.N., Gupta, V.K., and Bachheti, N. Fullerene-C60-modified electrode as a sensitive voltammetric sensor for detection of nandrolone—An anabolic steroid used in doping. Analytica Chimica Acta 2007. **597**: 82-89.

[14] Yue, Y., Hu, G., Zheng, M., Guo, Y., Cao, J., and Shao, S. A mesoporous carbon nanofiber-modified pyrolytic graphite electrode used for the simultaneous determination of dopamine, uric acid, and ascorbic acid. Carbon 2012. **50**: 107-114.

[15] Habibi, B., Abazari, M., and Pournaghi-Azar, M.H. A carbon nanotube modified electrode for determination of caffeine by differential pulse voltammetry. Chinese Journal of Catalysis 2012. **33**: 1783-1790.

[16] Zhao, S., Li, C., Huang, H., Liu, Y., and Kang, Z. Carbon nanodots modified cobalt phosphate as efficient electrocatalyst for water oxidation. Journal of Materiomics 2015. **1**: 236-244.

[17] Balandin, A.A., et al. Superior thermal conductivity of single-layer graphene. Nano Letters 2008. **8**: 902-907.

[18] Geim, A.K. and Novoselov, K.S. The rise of graphene. Nature Materials 2007. **6**: 183-191.

[19] Pei, S. and Cheng, H.-M. The reduction of graphene oxide. Carbon 2012. **50**: 3210-3228.

[20] Stankovich, S., Piner, R.D., Chen, X., Wu, N., Nguyen, S.T., and Ruoff, R.S. Stable aqueous dispersions of graphitic nanoplatelets via the reduction of exfoliated graphite oxide in the presence of poly(sodium 4-styrenesulfonate). Journal of Materials Chemistry 2006. **16**: 155-158.

[21] Schniepp, H.C., et al. Functionalized single graphene sheets derived from splitting graphite oxide. The Journal of Physical Chemistry B 2006. **110**: 8535-8539.

[22] An, S.J., et al. Thin film fabrication and simultaneous anodic reduction of deposited graphene oxide platelets by electrophoretic deposition. The Journal of Physical Chemistry Letters 2010. **1**: 1259-1263.

[23] Fuente, J.d.L. Reduced graphene oxide - what is it? How is it created? 2013. Available from: http://www.graphenea.com/pages/reduced-graphene-oxide#.VrBMBrJ97IU [2015, December 20]

[24] Kudin, K.N., Ozbas, B., Schniepp, H.C., Prud'homme, R.K., Aksay, I.A., and Car, R. Raman spectra of graphite oxide and functionalized graphene sheets. Nano Letters 2008. **8**: 36-41.

[25] Raj, M.A. and John, S.A. Fabrication of electrochemically reduced graphene oxide films on glassy carbon electrode by self-assembly method and their electrocatalytic application. The Journal of Physical Chemistry C 2013. **117**: 4326-4335.

[26] Chen, L., Tang, Y., Wang, K., Liu, C., and Luo, S. Direct electrodeposition of reduced graphene oxide on glassy carbon electrode and its electrochemical application. Electrochemistry Communications 2011. **13**: 133-137.

[27] Fan, Y., Liu, Y., Cai, Q., Liu, Y., and Zhang, J. Synthesis of CTAB-intercalated graphene/polypyrrole nanocomposites via in situ oxidative polymerization. Synthetic Metals 2012. **162**: 1815-1821.

[28] Mao, Y., Fan, Q., Li, J., Yu, L., and Qu, L.-b. A novel and green CTAB-functionalized graphene nanosheets electrochemical sensor for Sudan I determination. Sensors and Actuators B: Chemical 2014. **203**: 759-765.

[29] Ma, X., Chao, M., and Wang, Z. Electrochemical determination of Sudan I in food samples at graphene modified glassy carbon electrode based on the

enhancement effect of sodium dodecyl sulphonate. Food Chemistry 2013. **138**: 739-744.

[30] Hu, C. and Hu, S. Electrochemical characterization of cetyltrimethyl ammonium bromide modified carbon paste electrode and the application in the immobilization of DNA. Electrochimica Acta 2004. **49**: 405-412.

[31] Wen, X.-L., Jia, Y.-H., and Liu, Z.-L. Micellar effects on the electrochemistry of dopamine and its selective detection in the presence of ascorbic acid. Talanta 1999. **50**: 1027-1033.

[32] Manisankar, P., Selvanathan, G., and Vedhi, C. Determination of pesticides using heteropolyacid montmorillonite clay-modified electrode with surfactant. Talanta 2006. **68**: 686-92.

[33] Bard, A.J. and Faulkner, L.R. Electrochemical methods fundamentals and applications. John Wiley & Sons, Inc., 2001.

[34] Perez, F.R., BasÁez, L., Belmar, J., and Vanysek, P. Cyclic voltammetry of 1-(N-hexyl)-3-methyl-5-pyrazolone-based enamines and their chloromanganese(III) and nitridomanganese(V) complexes. Journal of the Chilean Chemical Society 2005. **50**: 575-580.

[35] Daneshegar, P., Moosavi-Movahedi, A.A., Norouzi, P., Ganjali, M.R., Farhadi, M., and Sheibanid, N. Characterization of paracetamol binding with normal and glycated human serum albumin assayed by a new electrochemical method. Journal of the Brazilian Chemical Society 2012. **23**: 315-321.

[36] Pradeep, T. Textbook of nanoscience and nanotechnology. McGraw-Hill Professional, 2012.

[37] Liu, Q., Shi, J., and Jiang, G. Application of graphene in analytical sample preparation. TrAC Trends in Analytical Chemistry 2012. **37**: 1-11.

[38] Novoselov, K.S., et al. Electric field effect in atomically thin carbon films. Science 2004. **306**: 666-669.

[39] Stoller, M.D., Park, S., Zhu, Y., An, J., and Ruoff, R.S. Graphene-based ultracapacitors. Nano Letters 2008. **8**: 3498-3502.

[40] Park, S. and Ruoff, R.S. Chemical methods for the production of graphenes. Nature Nanotechnology 2009. **4**: 217-224.

[41] Banks, C.E., Crossley, A., Salter, C., Wilkins, S.J., and Compton, R.G. Carbon nanotubes contain metal impurities which are responsible for the "electrocatalysis" seen at some nanotube-modified electrodes. Angewandte Chemie International Edition 2006. **45**: 2533-2537.

[42] Loh, K.P., Bao, Q., Eda, G., and Chhowalla, M. Graphene oxide as a chemically tunable platform for optical applications. Nature Chemistry 2010. **2**: 1015-1024.

[43] Guo, S. and Dong, S. Graphene nanosheet: synthesis, molecular engineering, thin film, hybrids, and energy and analytical applications. Chemical Society Reviews 2011. **40**: 2644-2672.

[44] Zhu, Y., et al. Graphene and graphene oxide: Synthesis, properties, and applications. Advanced Materials 2010. **22**: 3906-3924.

[45] Chua, C.K. and Pumera, M. Chemical reduction of graphene oxide: a synthetic chemistry viewpoint. Chemical Society Reviews 2014. **43**: 291-312.

[46] Stankovich, S., et al. Synthesis of graphene-based nanosheets via chemical reduction of exfoliated graphite oxide. Carbon 2007. **45**: 1558-1565.

[47] Zhang, J., Yang, H., Shen, G., Cheng, P., Zhang, J., and Guo, S. Reduction of graphene oxide vial-ascorbic acid. Chemical Communications 2010. **46**: 1112-1114.

[48] Yang, Z.Z., Zheng, Q.B., Qiu, H.X., Li, J., and Yang, J.H. A simple method for the reduction of graphene oxide by sodium borohydride with CaCl2 as a catalyst. New Carbon Materials 2015. **30**: 41-47.

[49] Fan, Z.J., et al. Facile synthesis of graphene nanosheets via fe reduction of exfoliated graphite oxide. ACS Nano 2011. **5**: 191-198.

[50] Wu, Z.S., Ren, W.c., Gao, L.b., Liu, B.l., Jiang, C.b., and Cheng, H.M. Synthesis of high-quality graphene with a pre-determined number of layers. Carbon 2009. **47**: 493-499.

[51] McAllister, M.J., et al. Single sheet functionalized graphene by oxidation and thermal expansion of graphite. Chemistry of Materials 2007. **19**: 4396-4404.

[52] Zhu, Y., Murali, S., Stoller, M.D., Velamakanni, A., Piner, R.D., and Ruoff, R.S. Microwave assisted exfoliation and reduction of graphite oxide for ultracapacitors. Carbon 2010. **48**: 2118-2122.

[53] Cote, L.J., Cruz-Silva, R., and Huang, J. Flash reduction and patterning of graphite oxide and its polymer composite. Journal of the American Chemical Society 2009. **131**: 11027-11032.

[54] Zhou, M., et al. Controlled synthesis of large-area and patterned electrochemically reduced graphene oxide films. Chemistry – A European Journal 2009. **15**: 6116-6120.

[55] Lin, X., Hong, Q., Wu, X., Guo, L., and Xie, Z. Analysis of phenoxyl-type N-methylcarbamate pesticide residues in vegetables by capillary zone electrophoresis with pre-column hydrolysis and amperometric detection. Journal of Chromatographic Science 2008. **46**: 615-621.

[56] Getzin, L.W., Cogger, C.G., and Bristow, P.R. Simultaneous gas chromatographic determination of carbofuran, metalaxyl, and simazine in soils. Journal of Association of Official Analytical Chemists 1989. **72**: 361-4.

[57] Abad, A., et al. Determination of carbaryl, carbofuran and methiocarb in cucumbers and strawberries by monoclonal enzyme immunoassays and high-performance liquid chromatography with fluorescence detection: An analytical comparison. Journal of Chromatography A 1999. **833**: 3-12.

[58] Li, H., et al. Carbofuran poisoning detected by mass spectrometry of butyrylcholinesterase adduct in human serum. Journal of Applied Toxicology 2009. **29**: 149-155.

[59] Jourdan, S.W., Scutellaro, A.M., Fleeker, J.R., Herzog, D.P., and Rubio, F.M. Determination of carbofuran in water and soil by a rapid magnetic particle-based ELISA. Journal of Agricultural and Food Chemistry 1995. **43**: 2784-2788.

[60] Pundir, C.S. and Chauhan, N. Acetylcholinesterase inhibition-based biosensors for pesticide determination: A review. Analytical Biochemistry 2012. **429**: 19-31.

[61] Ni, Y., Qiu, P., and Kokot, S. Simultaneous voltammetric determination of four carbamate pesticides with the use of chemometrics. Analytica Chimica Acta 2005. **537**: 321-330.

[62] Wei, H., Sun, J.J., Wang, Y.M., Li, X., and Chen, G.N. Rapid hydrolysis and electrochemical detection of trace carbofuran at a disposable heated screen-printed carbon electrode. Analyst 2008. **133**: 1619-24.

[63] Pozo, M., Hernández, L., and Quintana, C. A selective spectrofluorimetric method for carbendazim determination in oranges involving inclusion-complex formation with cucurbit[7]uril. Talanta 2010. **81**: 1542-1546.

[64] Feeds, R.o.P.i.F.A.A. Codex alimentarius commission. 2000, World Health Organization: Codex Alimentarius Commission.

[65] Johnson I, E.L., C Atkinson, E Aldous. Proposed EQS for Water Framework Directive Annex VIII substances: carbendazim (For consultation). 2009, Water Framework Directive - United Kingdom Technical Advisory Group (WFD-UKTAG).

[66] Joos, P. and Rillaerts, E. Theory on the determination of the dynamic surface tension with the drop volume and maximum bubble pressure methods. Journal of Colloid and Interface Science 1981. **79**: 96-100.

[67] Washburn, E.R. and Dunning, H.N. The determination of diffusion coefficients by measurements of surface tension. Journal of the American Chemical Society 1951. **73**: 1311-1313.

[68] Koczo, K.S., J. M. Measurement of dynamic surface tension of surfactant solution with the drop volume method using an automatic drop detector. Periodica Polytechnica Chemical Engineering 1989. **33**: 269-274.

[69] Punrat, E., Maksuk, C., Chuanuwatanakul, S., Wonsawat, W., and Chailapakul, O. Polyaniline/graphene quantum dot-modified screen-printed carbon electrode for the rapid determination of Cr(VI) using stopped-flow analysis coupled with voltammetric technique. Talanta 2016. **150**: 198-205.

[70] Ruecha, N., Rangkupan, R., Rodthongkum, N., and Chailapakul, O. Novel paper-based cholesterol biosensor using graphene/polyvinylpyrrolidone/polyaniline nanocomposite. Biosensors and Bioelectronics 2014. **52**: 13-19.

[71] Thammasoontaree, N., Rattanarat, P., Ruecha, N., Siangproh, W., Rodthongkum, N., and Chailapakul, O. Ultra-performance liquid chromatography coupled with graphene/polyaniline nanocomposite modified electrode for the determination of sulfonamide residues. Talanta 2014. **123**: 115-121.

[72] Rodthongkum, N., Ruecha, N., Rangkupan, R., Vachet, R.W., and Chailapakul, O. Graphene-loaded nanofiber-modified electrodes for the ultrasensitive determination of dopamine. Analytica Chimica Acta 2013. **804**: 84-91.

[73] Promphet, N., Rattanarat, P., Rangkupan, R., Chailapakul, O., and Rodthongkum, N. An electrochemical sensor based on graphene/polyaniline/polystyrene nanoporous fibers modified electrode for simultaneous determination of lead and cadmium. Sensors and Actuators B: Chemical 2015. **207, Part A**: 526-534.

[74] Wang, M., Huang, J., Wang, M., Zhang, D., and Chen, J. Electrochemical nonenzymatic sensor based on CoO decorated reduced graphene oxide for the simultaneous determination of carbofuran and carbaryl in fruits and vegetables. Food Chem 2014. **151**: 191-7.

[75] Tan, X., et al. Electrochemical sensor based on molecularly imprinted polymer reduced graphene oxide and gold nanoparticles modified electrode for detection of carbofuran. Sensors and Actuators B: Chemical 2015. **220**: 216-221.

[76] Razzino, C.A., Sgobbi, L.F., Canevari, T.C., Cancino, J., and Machado, S.A.S. Sensitive determination of carbendazim in orange juice by electrode modified with hybrid material. Food Chemistry 2015. **170**: 360-365.

[77] Li, J. and Chi, Y. Determination of carbendazim with multiwalled carbon nanotubes-polymeric methyl red film modified electrode. Pesticide Biochemistry and Physiology 2009. **93**: 101-104.

[78] Luo, S., Wu, Y., and Gou, H. A voltammetric sensor based on GO–MWNTs hybrid nanomaterial-modified electrode for determination of carbendazim in soil and water samples. Ionics 2013. **19**: 673-680.

[79] França, R.F., de Oliveira, H.P.M., Pedrosa, V.A., and Codognoto, L. Electroanalytical determination of carbendazim and fenamiphos in natural waters using a diamond electrode. Diamond and Related Materials 2012. **27–28**: 54-59.

[80] Ashrafi, A.M.D., J.; Guzsvavy, V.; Svancara, I.; Petrovic, T. T., Purenovic, M.; Vytras K. Trace determination of carbendazim fungicide using adsorptive stripping voltammetry with a carbon paste electrode containing tricresyl phosphate. International Journal of Electrochemical Science 2012. **7**: 9717-9731.

[81] Noyrod, P., Chailapakul, O., Wonsawat, W., and Chuanuwatanakul, S. The simultaneous determination of isoproturon and carbendazim pesticides by

single drop analysis using a graphene-based electrochemical sensor. Journal of Electroanalytical Chemistry 2014. **719**: 54-59.

[82] Aoac manual for peer verified methods program 1993. Available from: www.pfigueiredo.org/Bromono2b.pdf [2015, December 20]

APPENDIX

VITA

Nontapol Akkarachanchainon was born in March 26, 1991 in Bangkok, Thailand. He received his Bachelor Degree of Science, majoring in chemistry from Chulalongkorn University, Bangkok, Thailand (2009-2013). He has expected graduation of Master Degree of Science, majoring in Analytical Chemistry from Chulalongkorn University, Bangkok, Thailand in 2016.

Patent Application

"ขั้วไฟฟ้าแกรฟีนสำหรับเป็นตัวรับรู้ทางเคมีไฟฟ้า และกรรมวิธีการเตรียม" was requested for patent application with application form No. 1601000423, dated January 26, 2016.

Poster Presentation

Nontapol Akkarachanchainon, Prannee Rattanawaleedirojn, Nadnudda Rodthongkum, Orawon Chailapakul, "Electrochemically reduced graphene oxide modified carbon electrode for pesticide determination." Pure and Applied Chemistry Conference 2016, BITEC, Bangkok, Thailand, February 9-11, 2016.

Proceeding

Nontapol Akkarachanchainon, Prannee Rattanawaleedirojn, Nadnudda Rodthongkum, Orawon Chailapakul, "Electrochemically reduced graphene oxide modified carbon electrode for pesticide determination." Proceedings of Pure and Applied Chemistry Conference 2016, BITEC, Bangkok, Thailand, February 9-11, 2016, pp 1306-1310.